MICROBIOLOGY

Colocalization and potential interactions of *Endozoicomonas* and chlamydiae in microbial aggregates of the coral *Pocillopora acuta*

Justin Maire[1]*, Kshitij Tandon[1], Astrid Collingro[2], Allison van de Meene[1], Katarina Damjanovic[3], Cecilie Ravn Gotze[1,3], Sophie Stephenson[3], Gayle K. Philip[4], Matthias Horn[2], Neal E. Cantin[3], Linda L. Blackall[1], Madeleine J. H. van Oppen[1,3]

Corals are associated with a variety of bacteria, which occur in the surface mucus layer, gastrovascular cavity, skeleton, and tissues. Some tissue-associated bacteria form clusters, termed cell-associated microbial aggregates (CAMAs), which are poorly studied. Here, we provide a comprehensive characterization of CAMAs in the coral *Pocillopora acuta*. Combining imaging techniques, laser capture microdissection, and amplicon and metagenome sequencing, we show that (i) CAMAs are located in the tentacle tips and may be intracellular; (ii) CAMAs contain *Endozoicomonas* (Gammaproteobacteria) and *Simkania* (Chlamydiota) bacteria; (iii) *Endozoicomonas* may provide vitamins to its host and use secretion systems and/or pili for colonization and aggregation; (iv) *Endozoicomonas* and *Simkania* occur in distinct, but adjacent, CAMAs; and (v) *Simkania* may receive acetate and heme from neighboring *Endozoicomonas*. Our study provides detailed insight into coral endosymbionts, thereby improving our understanding of coral physiology and health and providing important knowledge for coral reef conservation in the climate change era.

INTRODUCTION

Coral reefs are among the most important ecosystems on the planet because they constitute biodiversity hotspots (*1*), and provide many goods and services, including coastal protection and important industries such as tourism and fisheries (*2*). Scleractinian corals are foundation members of coral reefs, as their skeleton forms the reefs' three-dimensional structure that provides habitats for many reef-dwelling organisms and because they are the main primary producers on the reef. Corals rely on a wide range of microorganisms for their survival, including protists, bacteria, archaea, fungi, and viruses (*3*–*5*). Photosynthetic dinoflagellates of the Symbiodiniaceae family are by far the most studied coral-associated microorganisms. They are vital symbionts because they provide their hosts with most of their energy through the translocation of photosynthate (*6*). Some coral-associated bacteria also have roles that are critical to the coral host, such as protection against pathogens (*7*), and cycling of nitrogen and sulfur (*8*–*10*).

Bacteria can colonize all microhabitats in corals and are most abundant and diverse in the mucus and skeleton (*3*, *4*). Tissue-associated bacteria are much less studied (*9*, *11*), although some are known to form large, dense clusters termed cell-associated microbial aggregates (CAMAs). Initially described in the early 1980s, they were thought to be linked to coral disease in *Acropora palmata* (*12*, *13*). CAMAs have since been described in numerous cnidarian species, including hard corals, soft corals, and anemones, regardless of disease status, and are particularly common in the genera *Acropora*, *Pocillopora*, *Porites*, *Platygyra*, and *Stylophora* (*14*–*23*). Apart from their location and distribution within the coral host, knowledge on CAMAs is scarce, with a handful of studies applying taxon-specific histological techniques to identify bacteria residing in CAMAs (*16*, *19*, *23*, *24*), and only one recent study applying culture-independent genomics to assess their functional potential (*21*). These studies have shown that bacteria residing in CAMAs often belong to the *Endozoicomonas* genus, a widespread coral symbiont (*24*). Several genomes of *Endozoicomonas* cultured from corals have been sequenced (*10*, *25*, *26*), but the location of these strains within the coral host and their ability to form CAMAs was not assessed. Hence, a holistic understanding of coral-associated CAMAs is still lacking, despite the huge progress made in coral microbiome research in the past couple of decades.

Here, we provide a detailed characterization of CAMAs in the coral *Pocillopora acuta*, including their location, subcellular structure, transmission, community composition, and functional potential (fig. S1 and table S1). *P. acuta* is an asexual brooder and sexual broadcast spawner coral (*27*). It acquires bacteria both vertically, from the mother colony, and horizontally, from the environment (*28*). Associated bacterial communities are often dominated by *Endozoicomonas* (*28*, *29*), and CAMAs have been detected in asexually produced larvae, suggesting their vertical transmission in this species (*28*). Using a combination of fluorescence in situ hybridization (FISH), confocal laser scanning microscopy (CLSM), and transmission electron microscopy (TEM), we show that CAMAs are located in the epidermal layer in tentacle tips of *P. acuta* polyps and are likely intracellular. CAMAs were precisely excised with laser capture microdissection (LCM), and community composition analysis showed that they contain bacteria of the families Endozoicomonadaceae and Simkaniaceae, a member of the Chlamydiota phylum. Metagenomic analyses suggest that Endozoicomonadaceae may be beneficial not only to their coral host but also to Simkaniaceae present in adjacent CAMAs.

[1]School of BioSciences, The University of Melbourne, Parkville, VIC 3010, Australia. [2]Centre for Microbiology and Environmental Systems Science, University of Vienna, Vienna 1030, Austria. [3]Australian Institute of Marine Science, PMB No 3, Townsville, QLD 4810, Australia. [4]Melbourne Bioinformatics, The University of Melbourne, Parkville, VIC 3010, Australia.
*Corresponding author. Email: justin.maire@unimelb.edu.au

RESULTS AND DISCUSSION

CAMAs are located in *P. acuta*'s tentacles

P. acuta colonies were sampled from the field and reared in captivity over a 3-year period, during which time they asexually produced two successive generations of corals (fig. S2). The two latter generations were used for this study and are hereafter referred to as generations F1 and F2. To investigate the location of CAMAs within *P. acuta* polyps, we first conducted whole-mount FISH with a universal bacterial probe (EUB338-mix). CLSM images showed that CAMAs are present at the tip of the tentacles (Fig. 1, A to C), but not anywhere else in the polyp. This was the case for all three genotypes we sampled (fig. S2A): C2_12, R2_8, and F1_6. Nematocysts present in the tentacles displayed substantial nonspecific binding, as evidenced by the simultaneous use of an antisense probe (Fig. 1A). FISH and CLSM performed on polyp sections yielded the same pattern (Fig. 1, D and E). Analysis of adult offspring (F2 generation) samples also revealed a multitude of CAMAs at the tip of the tentacles (Fig. 1, F and G). Other cnidarian studies show no consistency of in situ locations across species, with CAMAs being found in tentacles (*18*, *20*, *21*), mesenteries (*12*, *14*), and sometimes in all tissue types (*22*). CAMAs were exclusively seen in the epidermis and are thus not in contact with Symbiodiniaceae cells (Fig. 1E), which exist in the gastroderm. Therefore, CAMA bacteria are more likely to interact with the coral animal than with the Symbiodiniaceae in *P. acuta*. CAMAs have only been detected in the epidermis in *Exaiptasia diaphana* (*18*, *20*) and *Stylophora pistillata* (*19*), while they colonize the gastrodermis in *Pocillopora verrucosa* (*19*), *S. pistillata* (*14*, *15*, *19*), *Acropora aspera* (*15*), and *Acropora formosa* (*14*). This variability in location suggests that CAMAs may play distinct roles across coral holobionts. In addition, distinct infection mechanisms may exist and allow different bacterial taxa to colonize and aggregate in different tissues, e.g., tentacles may be a privileged site of contact between the coral and environmental bacteria.

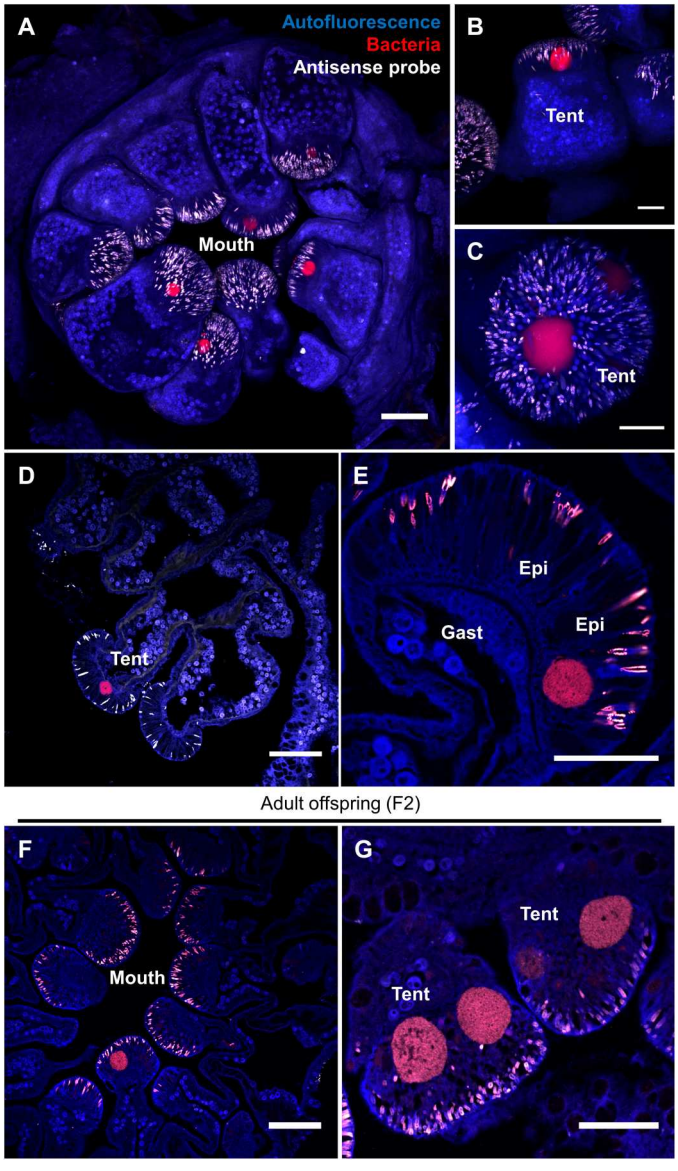

Fig. 1. CAMAs are located in the epidermis of *P. acuta*'s tentacles. (**A** to **C**) CAMA location by whole-mount FISH and CLSM in a whole adult polyp (A, maximum projection of a z-stack) and tentacles (B and C). (**D** to **G**) CAMA location by FISH on sectioned adult polyps. Genotypes: R2_8 (A and B), F1_6 (C, E, and F), and C2_12 (D and G). Generation: F1 (A to E) and F2 (F and G). Blue, autofluorescence; red, EUB338-mix probe (all bacteria); white, non-EUB probe (negative control). Gast, gastrodermis; Epi, epidermis; Tent, tentacle. Scale bars, 100 μm (A, D, and F) and 50 μm (B, C, E, and G).

While CAMAs are consistently found within cnidarian tissues, whether they are intra- or extracellular varies; they are intracellular in *E. diaphana* (*20*), extracellular in *A. palmata* (*13*), and both intra- and extracellular in *Porites compressa* (*23*). TEM images revealed that CAMAs are densely packed with bacteria (Fig. 2, A and B), which all show similar morphology and a highly visible nucleoid region (Fig. 2, C and D). TEM images in a previous study also showed the presence of nucleoid regions in CAMA bacteria (*20*). We observed a membrane encasing the CAMAs (Fig. 2, C and D, and fig. S3). While we only observed CAMAs in the C2_12 genotypes, three CAMAs were analyzed in this genotype, and all were surrounded by a membrane. This membrane resembled other coral cell membranes (Fig. 2C and fig. S3, A and F; see, for example, the membrane of a cnidocyte, surrounding a nematocyst in fig. S3E) and was composed of lipid bilayers (fig. S3D). This suggests that CAMAs are intracellular in *P. acuta*. It is possible that CAMAs are encased inside a vacuole, inside a coral cell. This is supported by the presence of eukaryotic content near CAMAs (e.g., Golgi apparatus in Fig. 2D) and the presence of a second membrane seemingly surrounding the CAMA membrane (Fig. 2C and fig. S3, A to C and F), sometimes fusing with the CAMA membrane (fig. S3, A and C). Alternatively, CAMAs may be extracellular, i.e., in between coral cells, and contained in a membrane of prokaryotic origin, or encased within a host-derived invasome (*30*). 4′,6-Diamidino-2-phenylindole (DAPI) staining combined with FISH showed the presence of one or more nuclei within CAMAs (Fig. 2, E and F), which is consistent with an intracellular nature. We also observed CAMAs that seemed to be disintegrating, with bacteria of a similar morphology seen outside the CAMAs (Fig. 2F). While this could be a sectioning or sample preparation artifact, it is also possible that CAMAs are dynamic within the coral holobiont and may be able to form and deform after colonization of the animal. The mechanisms by which these bacteria aggregate, and whether the process is controlled by the host, bacteria, or both, require further investigation.

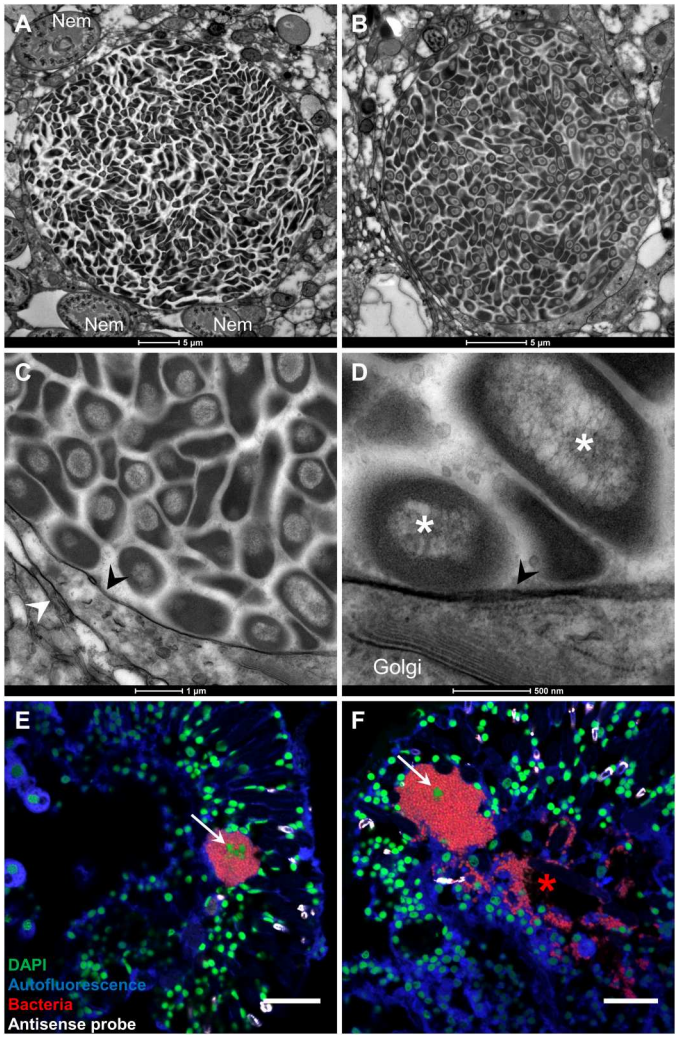

Fig. 2. CAMAs may be intracellular. (**A** to **D**) Subcellular structure of CAMAs observed in TEM. Black arrowheads point at a possible membrane surrounding the CAMAs. White arrowheads point at possible coral cell membranes. White asterisks show dense nucleoid regions of bacteria. (**E** and **F**) Combined FISH and DAPI staining observed by CLSM on sectioned adult polyps. White arrows point at host nuclei inside CAMAs. The red asterisk highlights a zone where bacteria are outside a CAMA. All images are from F1 generation samples. Genotype: C2_12 (A to E) and F1_6 (F). Blue, autofluorescence; red, EUB338-mix probe (all bacteria); white, non-EUB probe (negative control); green, DAPI. Scale bars, 20 µm (E and F). Nem, nematocysts.

Endozoicomonadaceae and Simkaniaceae are the main CAMA members

Using LCM, we specifically sampled CAMAs from two successive generations (F1 and F2; fig. S2A) of adult coral colonies belonging to the F1_6 genotype (fig. S4), which were raised entirely under controlled experimental conditions. 16*S* ribosomal RNA (rRNA) gene metabarcoding was performed to investigate the taxonomy of the bacteria contained in CAMAs. Sequencing statistics for this and the following metabarcoding experiments are summarized in table S2. Fourteen amplicon sequence variants (ASVs) were detected, although only 5 had a relative abundance above 0.1% in at least one sample (table S3A). Four of those were assigned to the *Endozoicomonas* genus, were present in all samples, and amounted to more than 95% of all reads (Fig. 3A). ASV01, ASV02, and ASV03 showed >99% identity with each other (fig. S5), suggesting that they might belong to a single *Endozoicomonas* species, while ASV04 was more distant (~96% identity to ASV01, ASV02, and ASV03) and is likely a separate species. A shift in relative abundance was observed between F1 and F2 generations, with ASV01 and ASV02 decreasing and ASV03 and ASV04 increasing, but the cause for this shift is unknown. While coral-associated bacterial communities can be different in captive compared to wild corals (*31*, *32*), *Endozoicomonas* often persists at high relative abundances in captive corals (*31*–*33*), as is the case in our study.

FISH using a previously published *Endozoicomonas* probe (*16*) confirmed that *Endozoicomonas* are present in the CAMAs (Fig. 3, B to E). Simultaneous use of the *Endozoicomonas* probe with a

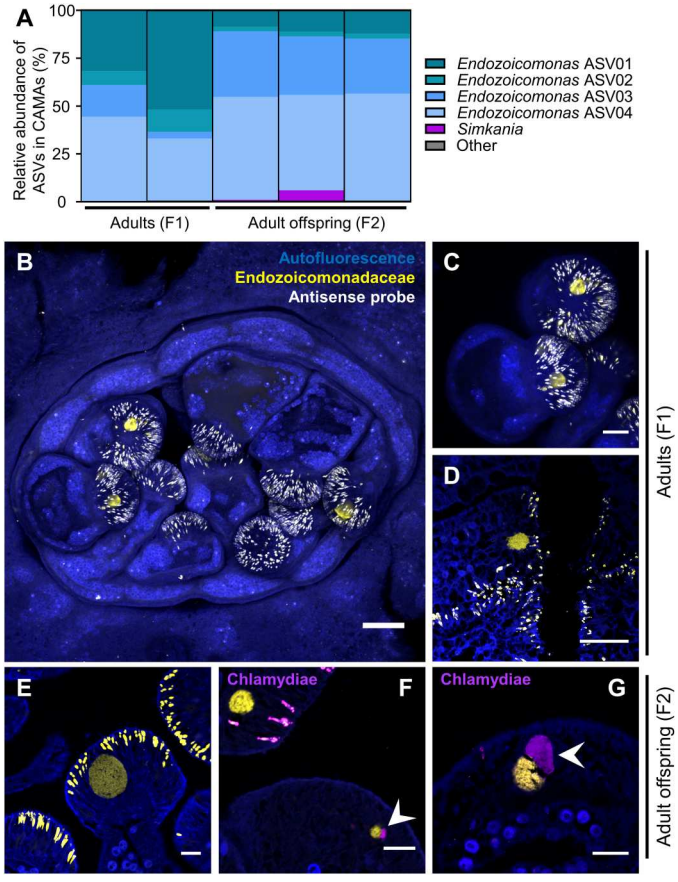

Fig. 3. CAMAs of the F1_6 genotype are composed of *Endozoicomonas* and *Simkania*. (**A**) Relative abundance of bacterial ASVs in CAMAs of adult polyps (F1_6 genotype, F1 and F2 generation) isolated by LCM. Each bar is a single replicate from one coral branch. ASVs classified as "Other" represent less than 0.1% of the communities and cannot be seen in the figure. Detailed composition is available in table S3. (**B** and **C**) Location of *Endozoicomonas* in CAMAs by whole-mount FISH in a whole adult polyp (B, maximum projection of a z-stack) and tentacle (C). (**D** to **G**) Location of *Endozoicomonas* and *Simkania* in CAMAs by FISH on sectioned adult polyps. White arrowheads point at *Simkania* CAMAs (purple), adjacent to *Endozoicomonas* CAMAs (yellow). All photos are from the F1_6 genotype. Generation: F1 (B to D) and F2 (E to G). Blue, autofluorescence; yellow, End663 probe (Endozoicomonadaceae); magenta, Chls523 probe (chlamydiae). Scale bars, 100 µm (B), 50 µm (C and D), and 25 µm (E and F).

universal bacterial probe showed complete colocalization (fig. S6A), confirming that *Endozoicomonas* are the main, and likely only, bacteria making up these CAMAs. FISH using the same probe has previously shown the presence of *Endozoicomonas* in CAMAs of *S. pistillata* and *P. verrucosa* (*16*, *19*, *24*), suggesting that *Endozoicomonas* commonly forms CAMAs in a range of coral species. Endozoicomonadaceae also form aggregates in the tissues of ascidians and fish (*34*, *35*), and inside the nuclei of mussel cells (*36*), suggesting that a conserved mechanism across this bacterial family may allow them to form aggregates inside animal hosts. Recently, Wada *et al.* (*21*) also used LCM to sample single CAMAs and confirmed with 16*S* rRNA gene metabarcoding the presence of two to three *Endozoicomonas* strains within individual CAMAs of *S. pistillata*. Because we pooled many CAMAs in our samples and used a genus-wide *Endozoicomonas* FISH probe, we cannot assess whether several strains co-occur in a single CAMA in *P. acuta*. The co-occurrence of two or more *Endozoicomonas* strains in CAMAs is puzzling and suggests that they might interact with one another. It also raises the question of strain compatibility and whether all *Endozoicomonas* strains can coexist within a CAMA.

The last ASV with a relative abundance over 0.5% was assigned to the *Simkania* genus (Fig. 3A) and was present in just two samples, both belonging to the F2 generation. The Simkaniaceae family belongs to the Chlamydiota phylum, which are obligate intracellular bacteria infecting a vast array of animals and thriving as symbionts of protists in diverse environments (*37*). Simkaniaceae ASVs are often detected at high relative abundances in coral samples (*21*, *32*, *38*), as well as in Symbiodiniaceae cultures (*39*, *40*), although their roles, as well as the cells they infect, remain uninvestigated. In the present study, FISH using a previously published chlamydiae probe (*41*), simultaneously with the *Endozoicomonas* probe, showed that *Simkania* inclusions are distinct from, but always adjacent to, *Endozoicomonas* CAMAs in *P. acuta* (Fig. 3, F and G). Use of the chlamydiae probe combined with the universal bacterial probe confirmed that *Simkania* occur alone within their inclusions (fig. S6B). The low relative abundance of *Simkania* in F1_6, its absence in three of five samples, and the low numbers of *Simkania* inclusions observed in FISH suggest that they might be opportunistic, like many other chlamydiae, rather than mutualistic. Additional sampling is needed to confirm whether *Simkania* commonly occurs as CAMAs in *P. acuta*, and to assess whether they form CAMAs in other coral species. While this is the first evidence of *Simkania* inclusions in corals, use of the Gimenez stain has previously suggested the presence of *Chlamydia*- or *Rickettsia*-like bacteria inclusions in *Acropora muricata* (*23*). Because chlamydiae are intracellular bacteria, the presence of *Simkania* inclusions reinforces the hypothesis that CAMAs are intracellular. Chlamydiae are known to co-occur with other bacteria in *Acanthamoeba* cells (*42*), although whether *Simkania* and *Endozoicomonas* share the same *P. acuta* cells is unclear. The close spatial proximity of the two types of clusters suggests that the different bacterial species may be interacting within the coral holobiont. Both *Endozoicomonas* and chlamydiae are fish pathogens, forming cysts in the gills and skin and negatively affecting breathing (*43*). Such cysts strongly resemble CAMAs, although there is no record of *Endozoicomonas* and chlamydiae infecting the same fish hosts.

CAMA bacteria exhibit mixed-mode transmission

The presence of CAMAs and of all four *Endozoicomonas* ASVs in both the F1 and F2 generations shows that this symbiotic association persists across generations and may be vertically transmitted to asexually produced larvae. However, we were not able to observe any CAMAs in freshly released F2 larvae (fig. S7). Because we may miss CAMAs when only looking at sections, we further conducted 16*S* rRNA gene metabarcoding on whole larvae of the F1_6 genotype to assess the presence of *Endozoicomonas* (table S2). Of the 179 ASVs detected in these samples, none were assigned to the *Endozoicomonas* genus or to the Endozoicomonadaceae family (table S4), suggesting the larvae do not contain CAMAs or *Endozoicomonas*. This suggests that *Endozoicomonas* are acquired horizontally in the F1_6 genotype, at the recruit or adult stage. Because F1 and F2 generation corals were kept in the same tank, it is likely that F1 colonies were the source of transmission. This contrasts with previous data showing the presence of CAMAs and of *Endozoicomonas* in larvae of distinct *P. acuta* genotypes sampled from Orpheus Island (*28*). Additional research on different genotypes, from a wider geographic distribution, sampled both in the wild and in captivity are therefore needed to clarify the mode of transmission of *Endozoicomonas*.

The *Simkania* ASV detected in the F2 adult samples of the F1_6 genotype was detected in every whole larval sample of the same genotype, with relative abundances ranging from 0.2 to 0.9% (table S4). This suggests that *Simkania* is transmitted to asexually produced larvae in the F1_6 genotype, and that CAMAs containing *Simkania* may have been missed when sampling the F1 generation adult samples. *Endozoicomonas* is likely to have a free-living life stage (*44*), while *Simkania* may be obligate symbionts. This is expected for *Simkania*, as all described chlamydiae depend on a eukaryotic host for propagation. These different transmission modes are likely to have affected the genome evolution and host-microbe interactions.

CAMA bacteria belong to undescribed *Endozoicomonas* and *Simkania* species

To assemble the genomes and investigate the functional potential of uncultured CAMA bacteria, metabarcoding samples were used for shotgun sequencing and metagenomic analyses. Three metagenome-assembled genomes (MAGs) were recovered, one from the F1 generation sample and two from the F2 generation samples. MAG data are detailed in Table 1. One MAG from each generation was assigned to *Endozoicomonas* (Pac_F1 and Pac_F2a), while the second MAG from the F2 generation sample was assigned to *Simkania* (Pac_F2b), consistently with our metabarcoding results. Pac_F1 and Pac_F2a genome sizes are similar to other *Endozoicomonas* genomes (*10*, *25*, *26*), while Pac_F2b is substantially smaller, which is consistent with its classification as a member of the intracellular chlamydiae (*45*). Pac_F2b′s genome size is like other animal-associated chlamydiae (1 to 1.5 Mb), whereas protist-associated chlamydiae usually have larger genomes (2 to 3 Mb) (*45*).

Because *Endozoicomonas* are so widespread in marine invertebrates, and particularly corals (*24*), we assessed their taxonomic placement. A full-length 16*S* rRNA gene [1536 base pairs (bp)] was recovered from Pac_F2a, and two nonoverlapping partial sequences were retrieved from Pac_F1 (401 and 1129 bp, respectively). ASV01 and ASV04 had 100% identity with Pac_F1 (1129-bp fragment) and Pac_F2a, respectively. A phylogenetic tree based on more

Table 1. Summary of the three metagenome-assembled genomes recovered in CAMAs sampled from adults of the F1_6 genotype. tRNAs, transfer RNAs.

MAG	Pac_F1	Pac_F2a	Pac_F2b
Genus assigned by GTDB-Tk	*Endozoicomonas*	*Endozoicomonas*	*Simkania*
Size (bp)	6,938,003	5,907,264	1,247,175
Coverage (mean value)	2,063.5×	3,539×	500.7×
Completeness (%)	94.25	88.76	88.02
Contamination (%)	1.65	2.48	0.21
G+C content (%)	49	51.3	43.9
N50	6,009	6,281	41,614
L50	314	248	12
Number of contigs	1,770	1,443	47
Number of coding sequences (CDS)	5,947	5,256	1,074
Number of rRNAs	10	5	1
Number of tRNAs	41	50	34

than 1000 Endozoicomonadaceae 16*S* rRNA gene sequences shows that our two strains cluster together with other *Endozoicomonas* strains isolated from *Pocillopora damicornis* (*46*) and *S. pistillata* (*16*, *21*) corals (fig. S8). This indicates a certain degree of host specialization in the Pocilloporidae family (*21*). However, this contrasts with other animal-*Endozoicomonas* associations, with host phylogenies rarely matching symbiont phylogenies (*21*, *25*, *26*), which is further evidence that *Endozoicomonas* have a free-living life stage and are not obligate symbionts. Pac_F1 and Pac_F2a form a well-supported clade together with *E. acroporae* (isolated from *Acropora* sp. corals), and to a lesser extent *E. atrinae* and *E. elysicola*, although they likely represent a previously undescribed species (~95 to 97% identity with *E. acroporae*, *E. atrinae*, and *E. elysicola*). A phylogenetic tree based on 120 bacterial gene markers from 15 *Endozoicomonas* genomes confirmed this trend (Fig. 4 and table S5A). Two clades were observed, with coral-associated *Endozoicomonas* present in both. Pac_F1 and Pac_F2a clustered together and were closest to two *Endozoicomonas* genomes recently sequenced from *S. pistillata* CAMAs (*21*). Average nucleotide identity (ANI) and average amino acid identity (AAI) showed strong similarity between Pac_F1 and Pac_F2a (98 and 96%, respectively) (fig. S9, A and B). The highest values were obtained with *Stylophora*-associated (ANI 83%, AAI 78%) and *Acropora*-associated (ANI 80%, AAI 70%) *Endozoicomonas*. Overall, these data suggest that Pac_F1 and Pac_F2a are two different strains that belong to an undescribed *Endozoicomonas* species, which is closely related to other Pocilloporidae-associated *Endozoicomonas*.

Only a partial 16*S* rRNA sequence (662 bp) was retrieved for Pac_F2b, so we created a phylogenetic tree based on 15 conserved marker genes, along with other chlamydiae and Simkaniaceae genomes (table S5B). As suggested by the GTDB-Tk classification, Pac_F2b falls in the same clade as *Simkania negevensis* and is closest to a MAG isolated from the coral *Cyphastrea* sp. sampled in subtropical Lord Howe Island (Australia) (Fig. 5 and fig. S10). AAI was highest with the MAG isolated from *Cyphastrea* sp. (75%) and *S. negevensis* (64%) (fig. S11). ANI values were too low (<75%) to be reliable. This suggests that Pac_F2b is an undescribed species that belongs to the *Simkania* genus. No host specificity was found, with Simkaniaceae associating with a wide range of hosts (Fig. 5).

Endozoicomonas may provide vitamins to its coral host and protect it against pathogens

The functional potential of the three MAGs recovered from CAMAs of *P. acuta* was investigated through Kyoto Encyclopedia of Genes and Genomes (KEGG), Rapid Annotations using Subsystems Technology (RAST), and InterProScan analyses and is summarized in Fig. 6. The completeness of selected KEGG pathways is provided in fig. S12. Detailed Prokka and eggNOG-mapper annotations are provided in dataset S1. We first focused on genes for host-symbiont interactions in the two *Endozoicomonas* MAGs, Pac_F1 and Pac_F2a (Fig. 6A). First, a total of nine secondary metabolites were bioinformatically predicted across the two MAGs (table S6). Only one showed similarity with a known biosynthetic gene cluster, which encodes the antibacterial protein rhizomide (*47*). The predicted secondary metabolites were also annotated by Prokka and were identified as antimicrobial proteins, such as gramicidin, tyrocidine, and microcin. In addition, several near-complete secretion systems were detected, including a type II, type III, and type VI (T2SS, T3SS, and T6SS, respectively). Note that a T6SS was only detected in Pac_F1. All three secretion systems may be involved in host infection and/or host cell entry, although their effectors remain unknown. While T2SSs and T3SSs are routinely observed in *Endozoicomonas* (*10*, *21*, *25*), this is only the second report of a T6SS in a coral-associated *Endozoicomonas* (*21*). These secretion systems, along with the secondary metabolites, may play a role in host colonization, outcompeting other bacteria present in the coral holobiont, as well as preventing other bacteria from invading CAMAs and promoting the maintenance of these structures. High numbers of genes encoding eukaryotic-like proteins were also detected (table S7), including more than 100 ankyrin-repeat proteins in each MAG. These are also found in other *Endozoicomonas* (*10*, *21*, *25*), are often effectors of secretion systems, and are hypothesized to facilitate host-bacteria interactions by mediating bacterial protein–eukaryotic host protein interactions (*48*). Last, both MAGs have the complete machinery to synthesize type IV pili (T4P). While never discussed in earlier publications, the pathway is also complete in other *Endozoicomonas* genomes (table S8). However, the gene encoding the actual pilus, *pilA*, is missing in *Parendozoicomonas haliclonae*. T4P are involved in bacterial motility and may play a role in host colonization, but they also support the formation of biofilms and aggregates (*49*). Specifically, *pilY1* encodes an adhesin that may be involved in host recognition. Therefore, we hypothesize that T4P are involved in the formation and maintenance of *Endozoicomonas* CAMAs. As *E. acroporae* forms CAMA-like structures in culture when incubated with dimethylsulfoniopropionate (DMSP) (*10*), it is possible that metabolic signals, such as DMSP, regulate the in hospite expression of T4P synthesis genes and, in turn, the formation of CAMAs.

Both *Endozoicomonas* MAGs encode pathways for the synthesis of several B vitamins, including thiamine (B_1), riboflavin (B_2), pyridoxin (B_6), biotin (B_7), and folate (B_9). Both corals and Symbiodiniaceae cannot produce B vitamins and are dependent on external

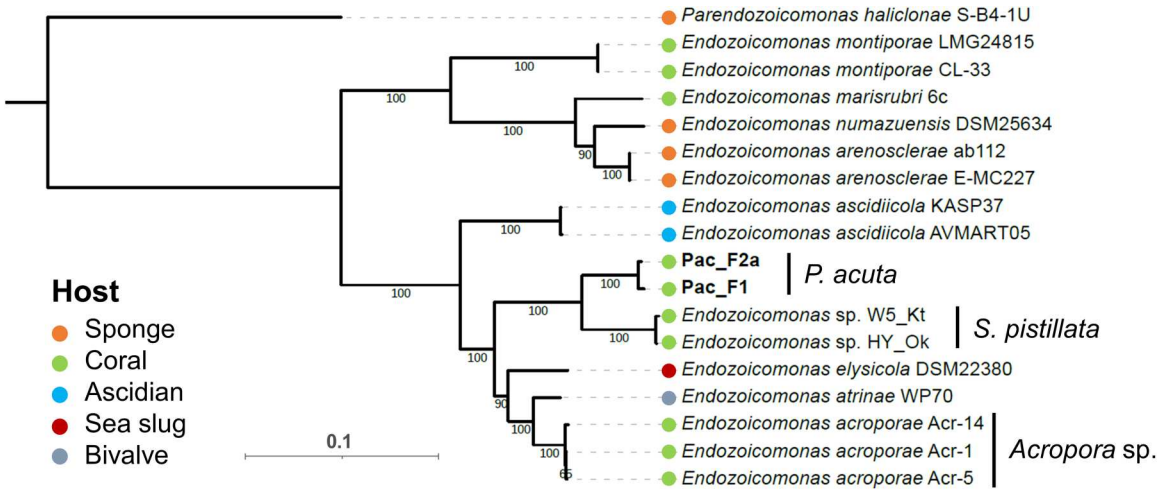

Fig. 4. Two MAGs sequenced from CAMAs belong to previously undescribed species of *Endozoicomonas*. Maximum likelihood phylogeny of *Endozoicomonas* based on 120 marker genes, 15 *Endozoicomonas* genomes, and 1 *Parendozoicomonas* genome (outgroup). Bootstrap support values based on 1000 replications are provided. Additional data on the reference genomes are available in table S5A.

sources. B vitamin provisioning from bacteria has been shown in hematophagous insects (*50*) and marine algae (*51*), and B vitamin synthesis pathways have been detected in other *Endozoicomonas* (*21*, *25*, *26*). Furthermore, thiamine and pyridoxin synthesis was up-regulated in *E. marisrubri* incubated with coral host extracts (*25*). It is therefore likely that *Endozoicomonas* provide B vitamins to its coral host and/or Symbiodiniaceae, although how these vitamins are exported remains elusive. As in other *Endozoicomonas* (*21*, *26*), we identified a wide range of ATP-Binding Cassette (ABC) transporters, notably for zinc, iron, amino acids, maltose, galactose, or heme. *Endozoicomonas* MAGs recently obtained from CAMAs in *S. pistillata* showed the presence of genes involved in phosphate transport, metabolism, and storage, as well as a phosphotransferase system, which led to the hypothesis that CAMAs may play a role in phosphate cycling and balance in the coral holobiont (*21*). Here, we only found genes encoding an ABC transporter for phosphate and a cellobiose phosphotransferase system, but no other genes that may suggest a role in phosphate metabolism. Last, we also detected several pathways for the synthesis of molecules involved in antioxidant processes, including lipoic acid, heme (incorporated into hemoproteins, such as catalases and peroxidases), and glutathione. Antioxidant synthesis is a trait of high interest in the design of bacterial probiotics for the mitigation of coral bleaching (*52*, *53*), as the overproduction of reactive oxygen species by Symbiodiniaceae is thought to be one of the main drivers of coral bleaching (*54*). Thus, *Endozoicomonas* is likely to be a beneficial symbiont for its host, potentially providing vitamins, antioxidants, and antimicrobial molecules.

Simkania may benefit from *Endozoicomonas* for growth and survival

The *Simkania* MAG Pac_F2b exhibited reduced metabolic abilities (Fig. 6B), which is consistent with other chlamydiae and their intracellular lifestyle (*45*). It has all the genes for glycolysis, the tricarboxylic acid (TCA) cycle, and the pentose phosphate pathway. In addition, Pac_F2b encodes the genes for the transformation of acetate into acetyl–coenzyme A (acetyl-CoA), potentially enabling this *Simkania* strain to use acetate as a substrate for the TCA cycle and as a carbon source (fig. S12). Acetate can be produced through glycolysis and pyruvate oxidation. In a similar way, sponge-associated chlamydiae can use acetoin as an energy source (*55*). Both *Endozoicomonas* MAGs can produce acetate via two pathways (fig. S13): (i) through the conversion of acetyl-CoA, produced by pyruvate oxidation, into acetate and (ii) through the conversion of DMSP into methylmercaptopropionate by DmdA, and subsequently into acetate. Not all the genes in the DMSP conversion pathway were found, which may be due to MAG incompleteness. Because acetate can freely diffuse across membranes, we hypothesize that excess acetate produced by *Endozoicomonas* present in neighboring CAMAs may be acquired by *Simkania* and be an additional carbon source for its own growth. Like most chlamydiae, Pac_F2b lacks the genes for de novo nucleotide biosynthesis and can only synthesize a small number of amino acids (alanine, aspartate, and glutamate), but has a complete shikimate pathway. Other hallmark chlamydial genes were detected, including a T3SS, adhesins, adenosine triphosphate (ATP)/adenosine diphosphate (ADP) translocases, and virulence effectors such as proteases and kinases (Fig. 6B). An orthogroup analysis revealed that 518 of Pac_F2b′s genes (almost 50%) were present in more than 90% of all publicly available chlamydial genomes and 204 genes were shared by two other *Simkania* genomes (dataset S2). This suggests that Pac_F2b′s overall genomic content is similar to that of other chlamydiae. In addition, the analysis uncovered 97 genes unique to Pac_F2b, but none could be annotated (dataset S3, A and B). Two unique genes (Pacuta_bin2_01330 and Pacuta_bin2_06340) showed high similarity with *Endozoicomonas* genes, particularly with the Pac_F1 MAG (dataset S3, C and D; each gene had a hit in Pac_F1 with >96% identity at the protein level). The two genes were annotated in other *Endozoicomonas* as a protein kinase and an RNA ligase, respectively. Both genes were present on contigs containing other chlamydial genes, suggesting that assembly/binning errors did not result in the presence of these genes in Pac_F2b. Therefore, this opens the possibility of horizontal gene transfer between *Endozoicomonas* and *Simkania*.

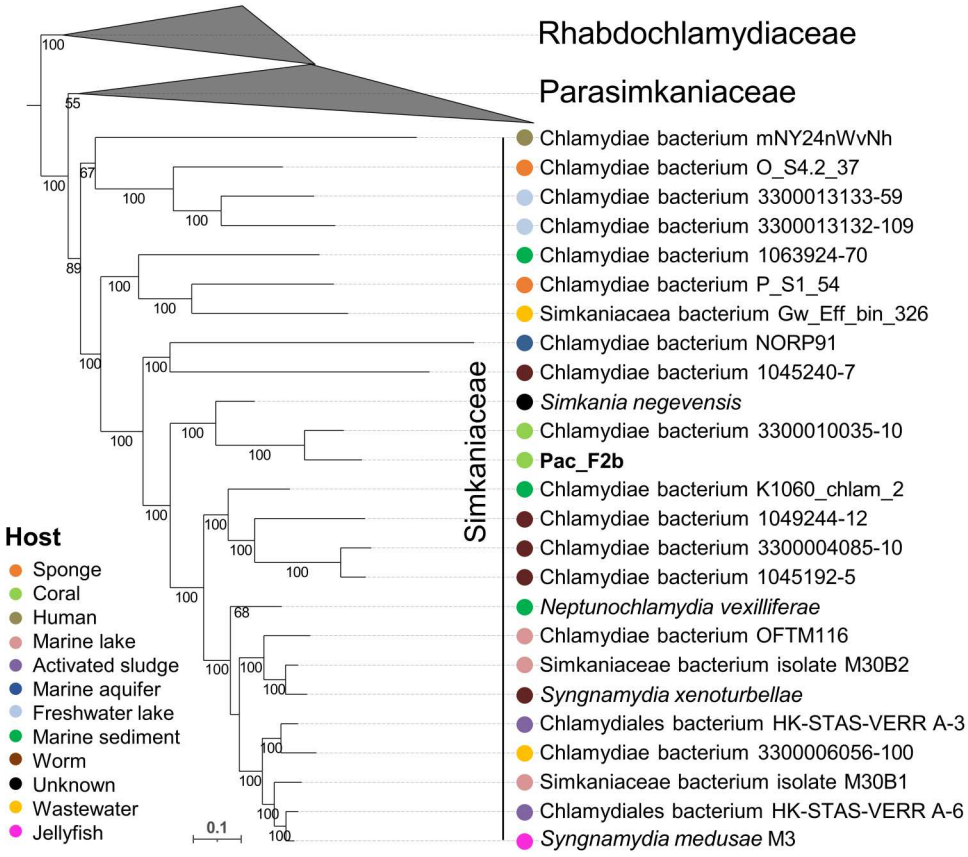

Fig. 5. One MAG sequenced from CAMAs belongs to a previously undescribed species of *Simkania*. Chlamydial maximum likelihood phylogeny based on 15 conserved NOGs in 24 Simkaniaceae, 8 Parasimkaniaceae, and 21 Rhabdochlamydiaceae (outgroup) genomes. Bootstrap support values based on 1000 replications are provided. Additional data on the reference genomes are available in table S5B. A tree containing the entire chlamydial phylogeny is available in fig. S10.

The only vitamin/cofactor Pac_F2b can produce is menaquinol, which is common in chlamydiae (*55*) and plays a role in bacterial growth in *Chlamydia trachomatis* (*56*). Pac_F2b may import other vitamins from host cells or adjacent *Endozoicomonas* through vitamin transporters such as BioY, present in Pac_F2b. Unlike most other chlamydiae (*55*), it does not encode the heme biosynthesis pathway. Although the genome sequence of the Pac_F2b MAG is not complete, it is highly unlikely that the full heme pathway is present. None of the heme biosynthesis genes could be detected in the closest relative, the *Cyphastrea*-associated Chlamydiae bacterium 3300010035-10, either, and these genes are scattered at six loci throughout the chromosome in *S. negevensis*. Heme is essential for many cellular processes, including antioxidant functions, as well as infectivity and virulence in many pathogens. For example, heme production is essential for the intracellular survival of *Brucella abortus* (*57*). Heme-deficient strains of *Staphylococcus aureus* show reduced tissue colonization in mice compared to wild-type strains (*58*), although they persist more easily intracellularly, perhaps because of lower toxin production (*59*). The specific role of heme in chlamydiae remains unknown, although mutations in the *hemG* gene, involved in heme synthesis, were associated with increased infectivity in *C. trachomatis* (*60*). In *P. acuta*, *Simkania* may acquire heme from the host. Alternatively, *Endozoicomonas* have the complete heme biosynthesis pathway and an ABC transporter for heme, suggesting that it is able to acquire iron from host tissues, synthesize heme, and export it. Neighboring *Simkania* may be able to take advantage of this and acquire heme synthesized by *Endozoicomonas*. However, no heme import system was detected in Pac_F2b and how heme would cross CAMA or *Simkania*'s membranes remains unclear. It is also possible that the lack of heme synthesis in Pac_F2b makes this strain less virulent and able to persist in inclusions in *P. acuta*, similarly to *S. aureus*.

In summary, it is possible that *Simkania* receives acetate from *Endozoicomonas*, which *Simkania* can use to stimulate its growth, as well as heme and vitamins. Interactions between bacteria within a holobiont are known in insects where endosymbiotic bacteria share a single cell, e.g., *Buchnera/Serratia* in the aphid *Cinara cedri* (*61*) or *Tremblaya/Moranella* in the mealybug *Planococcus citri* (*62*) (note that in the latter, *Moranella* resides within *Tremblaya* cells). In both cases, the synthesis of some amino acids requires a patchwork of genes present in one symbiont or the other. The potential metabolic interactions we uncovered in *P. acuta* may explain the spatial proximity of the two types of CAMAs, and why we did not observe any *Simkania* CAMAs on their own. Nevertheless, the presence of *Simkania* without *Endozoicomonas* in larvae samples of the F1_6 genotype (table S4) suggests that potential *Endozoicomonas-Simkania* interactions (heme/vitamin provisioning and acetate supplementation) are not necessary for *Simkania* survival. However, *Simkania* was in low relative abundance in these samples (<1%) and was not observed forming CAMAs (fig. S6).

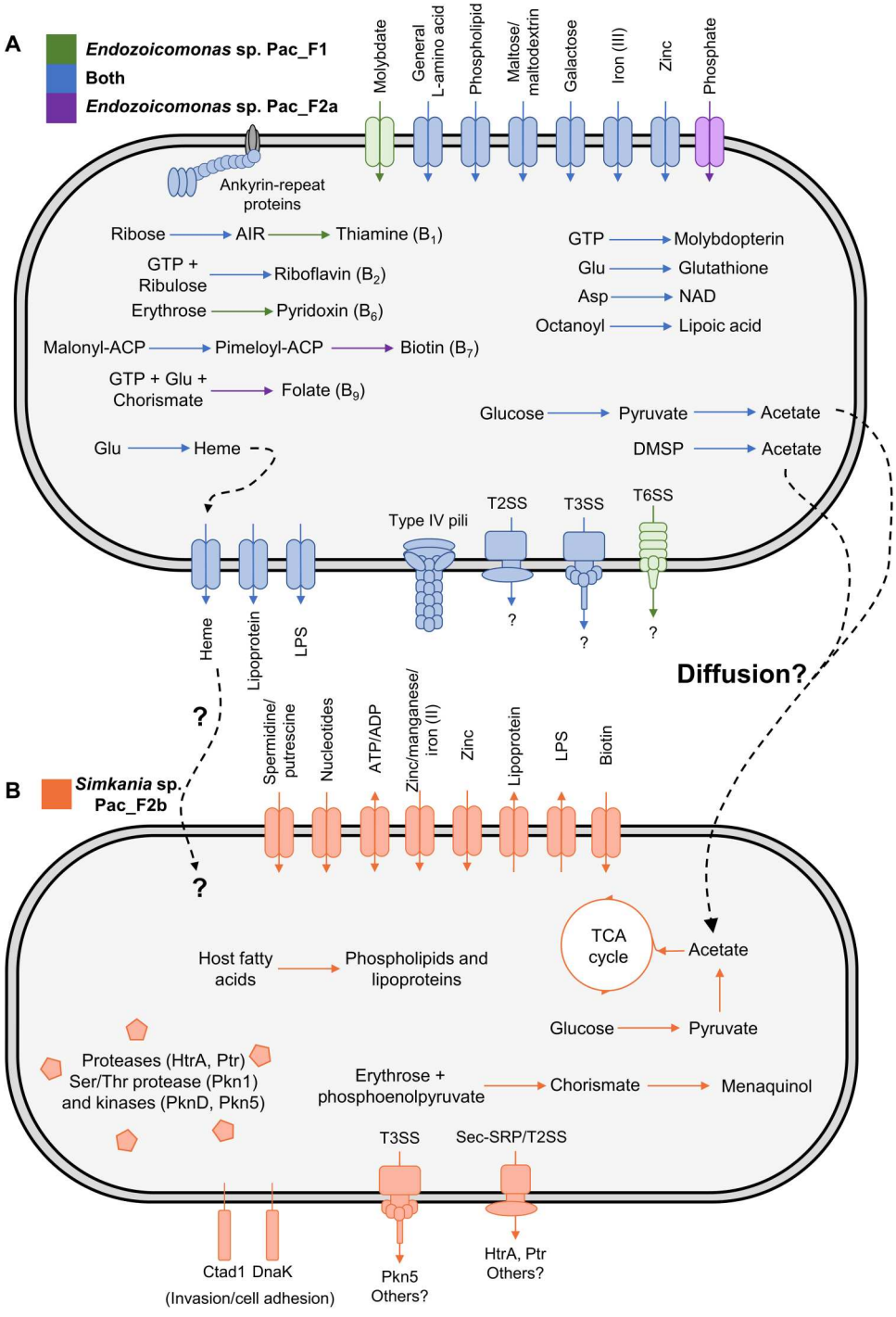

Fig. 6. Overview of the genomic potential of the three MAGs recovered from *P. acuta* CAMAs. The pathways represented here either are complete or only lack one gene (fig. S12) in *Endozoicomonas* sp. Pac_F1 (**A**) and Pac_F2a (A), or *Simkania* sp. Pac_F2b (**B**). Dashed arrows represent hypothetical interactions between *Endozoicomonas* and *Simkania* (fig. S13). Sec-SRP, Sec translocase and signal recognition particle pathway; T2SS, type II secretion system; T3SS, type III secretion system; T6SS, type VI secretion system; TCA, tricarboxylic acid; AIR, aminoimidazole ribotide; DMSP, dimethylsulfoniopropionate; LPS, lipopolysaccharide; NAD, nicotinamide adenine dinucleotide.

This suggests that either its growth is impeded or it is instead dependent on host-produced compounds. In the latter scenario, *Simkania* would not be restricted to aggregate around *Endozoicomonas* and may be able to source host compounds from different coral cell types, hence the absence of CAMAs in these samples. Simkaniaceae and Endozoicomonadaceae co-occur in corals of the *Acropora*, *Stylophora*, and *Pocillopora* genera (*21*, *32*, *38*, *63*). These corals cover the complex and robust clades within the Scleractinia. The interactions suggested by our genomic data may thus be widespread in coral holobionts and should be studied further.

We provide a comprehensive overview of the biology of CAMAs in the coral *P. acuta*. CAMAs are located at the tip of the tentacles, contain members of the *Endozoicomonas* and *Simkania* genera, and exhibit mixed-mode transmission, and genomic data suggest that they bear a wide range of functions, including an antagonistic effect toward other bacteria, and the production of B vitamins and antioxidants. This further establishes *Endozoicomonas* as a widespread mutualistic symbiont of corals, and we provide additional evidence that *Endozoicomonas* symbionts vary in their genetic potential and life strategies. The differences found in this study compared to previous research adds to the diversity of *Endozoicomonas*-coral interactions and reinforces the need for wider studies targeting additional coral species, from diverse geographical origins, both in captivity and in the field. Our findings provide spatial and genomic evidence for the concurrent occurrence of CAMAs composed of different microbes, suggesting interactions between CAMAs for bacterial and coral host functioning. Overall, our study unpicks the interactions between bacteria and corals, thereby enhancing our understanding of coral physiology and health. Such knowledge is critical in the climate change era and may help develop approaches for the mitigation of coral bleaching.

MATERIALS AND METHODS

Coral husbandry and aquarium conditions

For the F1_6, C2_12, and R2_8 genotypes, three parent colonies were collected from three reefs in July 2017 [permit from the Great Barrier Reef (GBR) Marine Park Authority G14/36732.1], Feather reef (colony ID: 202B F1_6; latitude: −17.51854, longitude: 146.38940), Coates reef (colony ID: 307A C2_12; latitude: −17.18850, longitude: 146.37180), and Rib reef (colony ID: 211D R2_8; latitude: −18.47122, longitude: 146.87360), along the central GBR in Australia (table S1 and fig. S2A). The colonies were brought back to the National Sea Simulator at the Australian Institute of Marine Science in Townsville, QLD, Australia. Parent colonies were kept in aquaria, running an annual temperature profile based on historical sea surface temperature (SST) records (1985–2012) for the mid-shelf central GBR obtained from National Oceanic and Atmospheric Administration (NOAA) Coral Reef Watch (CRW) daily global 5 km (0.05 degree) satellite product v3.1 (fig. S14). The annual temperature profile targeted an annual average temperature for the central GBR of 26.14 ± 0.23°C [±1 daily standard deviation (SD)], an annual range from 23.16° to 29.88°C, with a summer heat stress accumulation equivalent to 0.95°C weeks (NOAA CRW v3.1). Corals were maintained in a semi-recirculating system containing oceanic inshore seawater filtered to 0.04 μm. Daily turnover was ~300%, and circulation within tanks was achieved with two pumps (Maxspect 350 series) generating gyres at opposite ends of the tanks; partial CO_2 pressure was maintained at a daily average value 464 ± 40.94 parts per million (±1 daily SD) allowing for diurnal variability driven by natural photosynthesis and respiration cycles; daily light cycles were set to match local conditions with daily and seasonal variations in solar intensity and lunar cycles to maintain synchronicity of planulation patterns for *P. acuta* colonies. Corals were fed daily with freshly hatched *Artemia nauplii* and Shellfish Diet 1800 (Reed Mariculture, USA).

From July to October 2017, fully developed F1 larvae, released asexually by the parent colonies, were collected with flow-through collection devices on the outflow of isolation tanks and settled separately under constant temperature–controlled flow-through seawater onto preconditioned aragonite settlement plugs. From September 2018 to February 2019, F2 larvae, generated asexually by the F1 colonies (12 to 16 months old at that point), were collected with flow-through collection devices on the outflow of isolation tanks and settled separately under constant temperature–controlled flow-through seawater onto preconditioned aragonite settlement plugs. Throughout their life, both generations were kept in the same mesocosm systems under the same annual conditions as parent colonies.

Sampling

For adult colonies, small coral fragments were snapped off the colonies with forceps, rinsed with 0.22-μm filtered seawater (FSW), and placed in cryovials. Forceps were rinsed in 80% ethanol between sampling each colony. Two to three fragments per colony were placed in one cryovial. Three colonies were sampled per genotype. For FISH and LCM, branches were fixed for 24 hours in 4% paraformaldehyde (PFA) in 0.22-μm FSW, rinsed twice in FSW, and stored in 50% ethanol–phosphate-buffered saline (PBS) at −20°C. For TEM, branches were fixed for 24 hours in 4% PFA + 0.1% glutaraldehyde in FSW, rinsed once in FSW and once in 1× PBS, and stored in 1× PBS at 4°C. Following fixation, coral branches were decalcified in 10% EDTA. EDTA was renewed every 2 days, and samples were kept at 4°C on a rotating wheel, until there was no skeleton left (around 2 weeks). Samples were then rinsed in 1× PBS and stored at 4°C in 1× PBS. For FISH observations, six branches were sampled per genotype per generation (three for sectioning, three for whole-mount FISH). For TEM, one branch per genotype was sampled, although observations were ultimately only successful in one genotype. For LCM, three branches per generation of the F1_6 genotype were sampled. All replicates throughout the study are biological replicates.

Larvae were sampled as previously described (*28*). Briefly, before planulation, colonies of the F1 generation were maintained in individual acrylic aquaria that received indirect natural sunlight and coarsely filtered seawater. A filter was fitted at each outlet of the acrylic tank to collect released planulae. Each larva was washed with FSW transferred from the filter into an Eppendorf tube (FISH) or cryovial (metabarcoding) using a sterile pipette tip, and as much water as possible was removed without disturbing the larvae. For FISH, five larvae per genotype were sampled. For metabarcoding, 18 larvae of the F1_6 genotype were sampled in six tubes (three larvae per tube), immediately snap-frozen following sampling, and kept at −80°C.

FISH on slides

Sample processing, sectioning of larvae, and decalcification of branches were performed by the Melbourne Histology Platform (University of Melbourne). First, samples were dehydrated in 50% ethanol for 1 hour, 70% ethanol for 1 hour, 90% ethanol for 45 min, 100% ethanol for 1 hour (three times), 50% ethanol and 50% xylene for 45 min, xylene for 45 min (twice), and paraffin for 50 min (three times). Samples were subsequently embedded in solid paraffin, and 3-µm sections were cut using a Microm HM 325 rotary microtome and plain microscopic slides (Menzel, Germany). Each slide had four serial sections. FISH was then performed as previously described (*28*), except the final probe concentration during hybridization was 5 ng/µl. See table S9 for probe sequences and formamide concentrations (*16*, *41*, *64*, *65*). Slides were mounted in CitiFluor CFM3 mounting medium (proSciTech, Australia) containing DAPI (3 µg/µl; Merck, Germany) to stain nucleic acids, covered with a coverslip, and sealed with clear nail polish. Slides were kept at 4°C until observation. For each genotype and generation, three branches were observed.

Whole-mount FISH

Single polyps were dissected in 1× PBS using Dumont tweezers under a dissecting microscope. Tissue was cleared of autofluorescence by incubating polyps in 50% methanol for 10 min, 75% methanol for 10 min, 90% methanol for 10 min, 100% methanol for 10 min, 90% methanol + 0.2% Triton X-100 for 10 min, 75% methanol + 0.2% Triton X-100 for 10 min, 50% methanol + 0.2% Triton X-100 for 10 min, and 1× PBS + 0.2% Triton X-100 for 10 min and stored at 4°C in 1× PBS.

The whole-mount FISH protocol was adapted from previously published protocols (*28*, *66*). Samples were first permeabilized in 70% acetic acid for 2 min and twice rinsed in 1× PBS for 5 min. Samples were then incubated in 1× PBS + 0.1% Triton X-100 for 10 min, 1× PBS for 5 min, pepsin at 0.2 mg/ml in 0.01 M HCl at 37°C for 30 min, 1× PBS for 5 min, 0.2 M HCl for 12 min, and 20 mM tris-HCl for 10 min. Hybridization was performed in the dark for 3 hours at 46°C in 2 ml of hybridization buffer [0.9 M NaCl, 20 mM tris-HCl (pH 7.2), 0.01% SDS, and 5 ng/ml of probe; see table S9 for formamide concentration]. A negative control with no probe was included. Samples were then washed for 15 min at 48°C in washing buffer [20 mM tris-HCl (pH 7.2) and 0.01% SDS; see table S9 for NaCl concentration]. Samples were then rinsed twice in ice-cold Milli-Q water and deposited onto eight-well coverslip-bottom slides (ibidi, USA). A drop of Milli-Q water was deposited onto each polyp to avoid drying. Slides were kept at 4°C until observation. For each genotype, five individual polyps were observed.

Confocal laser scanning microscopy

Slides were observed on a Nikon A1R confocal laser scanning microscope (Nikon, Japan) with the NIS325 Element software. Virtual band mode was used to acquire variable emission bandwidth to tailor acquisition for specific fluorophores. The fluorophores Cy3 and Atto550 were excited using the 561-nm laser line, Atto647 using the 640-nm laser line, DAPI using the 405-nm laser line, and the coral autofluorescence using the 488-nm laser line with a detection range of 570 to 620 nm for Cy3 and Atto550, 660 to 710 nm for Atto647, 500 to 550 nm for coral autofluorescence, and 420 to 480 nm for DAPI. For three-dimensional reconstructions of z-stacks (Figs. 1A and 3B), sections were acquired using Z steps of 3 µM with the 10× objective and 1.1 µM with the 20× objective. Nd2 files were processed using ImageJ. Linear adjustments of brightness and contrast were performed when necessary and applied to the entire image and to each channel independently. Channels were then merged together. Z-stacks were projected in two-dimensional images using the "Max Intensity" projection type.

Transmission electron microscopy

Following decalcification, single polyps were dissected in 1× PBS using Dumont tweezers under a dissecting microscope. Samples were washed in distilled water 3 × 10 min followed by postfixation with 1% osmium tetroxide in double-distilled water for 1 hour. Samples were then dehydrated in an acetone series of 10, 20, 40, 60, 80, and 100% acetone. Two further exchanges of 100% acetone were undertaken before infiltrating and embedding the samples in Spurr's resin. Thin (100-nm) sections were cut on a Leica UC7 ultramicrotome and collected on copper slot grids. The sections were poststained with 1% uranyl acetate in water for 10 min and 3% lead citrate for 2 min and imaged on an FEI Tecnai Spirit TEM equipped with an Eagle charge-coupled device camera (Thermo Fisher Scientific). CAMAs were only detected in one polyp of the C2_12 genotype.

LCM of CAMAs

Genotypes F1_6 (adults, generations F1 and F2) were chosen to perform LCM to extract CAMAs. For each group, three replicates containing one branch were processed. For each replicate, 10 slides each containing eight sections were processed (~80 sections per replicate in total). FISH was performed as described above, using the EUB388-mix–Atto550 probe. Slides were not mounted and left without coverslip. To check that FISH had worked and to take photos comparing before and after LCM, one slide per group was covered with a coverslip (without any mounting medium) and sealed with clear nail polish for CLSM imaging as described above. The nail polish was then carefully dissolved by applying small amounts of acetone with a cotton swab, and the coverslip was removed. All slides were processed by LCM the next day to avoid any loss of signal. LCM was performed on the PALM Laser Microdissector (Zeiss, Germany), using the PALM Robo 3.2 software, and a 20× air objective. CAMAs were detected using a tetramethyl rhodamine isothiocyanate filter (excitation, 550 ± 12.5 nm; emission, 605 ± 35 nm). Individual CAMAs were captured using an ultraviolet laser (355 nm) into the caps of 200-µl AdhesiveCap Clear tubes (Zeiss, Germany). These caps are filled with clear adhesive material that ensures sample retention. CAMAs from all slides from one replicate were all collected in one tube. For each replicate, tissue areas without CAMAs were also separately captured as a control. DNA extraction was then conducted within the cap, using the Arcturus PicoPure DNA Extraction Kit (Applied Biosystems, USA). Reconstitution buffer (155 µl) was added into one vial of proteinase K to dissolve the enzyme. Proteinase K solution (10 µl) was then added to each cap and incubated at 65°C for 18 hours. Tubes were then centrifuged for 5 min at 10,000*g* to bring samples down into the tubes and stored at −20°C. Two to three caps containing no sample, but that were open in the LCM facility to capture air contamination, were also included as extraction blanks.

DNA extractions of whole larvae

Six tubes each containing three larvae produced by F1 generation colonies of the F1_6 genotype were processed. DNA extractions were performed using a salting-out method as previously described (*67*). Three blank DNA extractions were conducted as negative controls. A mock community, ZymoBIOMICS Microbial Community DNA Standard (Zymo Research), was included to check sequencing and processing quality.

16*S* rRNA gene metabarcoding

Hypervariable regions V5-V6 of the 16*S* rRNA genes were amplified using the primer set 784F (5′-GTGACCTATGAACTCAGGAGTCAGGATTAGATACCCTGGTA-3′) and 1061R (5′-CTGAGACTTGCACATCGCAGCCRRCACGAGCTGACGAC-3′). Adapters were attached to the primers and are shown as underlined. Bacterial 16*S* rRNA genes were polymerase chain reaction (PCR)–amplified on the SimpliAmp Thermal Cycler (Applied Biosystems, Thermo Fisher Scientific). Each reaction contained 1 μl of DNA template, 1.5 μl of forward primer (10 μM stock), 1.5 μl of reverse primer (10 μM stock), 7.5 μl of 2× Multiplex PCR Master Mix (Qiagen, Germany), and 3.5 μl of nuclease-free water (Thermo Fisher Scientific), with a total volume of 15 μl per reaction. Three triplicate PCRs were conducted for each sample, and three no template PCRs were conducted as negative controls. PCR conditions for the 16*S* rRNA genes were as follows: initial denaturation at 95°C for 3 min and then 18 cycles of denaturation at 95°C for 15 s, annealing at 55°C for 30 s, and extension at 72°C for 30 s, with a final extension at 72°C for 7 min. Samples were then held at 4°C. Following PCR, triplicates were pooled, resulting in 45 μl per sample. Metabarcoding library preparation was conducted as previously described (*68*), and sequencing was performed at the Walter and Eliza Hall Institute in Melbourne, Australia on one MiSeq V3 system (Illumina) with 2 × 300 bp paired-end reads.

Bacterial 16*S* rRNA gene analysis

QIIME2 v2020.11 (*69*) was used for processing 16*S* rRNA gene sequences. The plug-in demux (*69*) was used to create an interactive plot to visualize the data and assess the quality, for demultiplexing and quality filtering of raw sequences. The plug-in cutadapt (*70*) was used to remove the primers and MiSeq adapters. Plug-in DADA2 (*71*) was used for denoising and chimera checking, trimming, dereplication, generation of a feature table, joining of paired-end reads, and correcting sequencing errors and removing low-quality reads (Q score < 30). Summary statistics were obtained using the feature-table to ensure that processing was successful. Taxonomy was assigned by training a naive Bayes classifier with the feature-classifier plug-in (*69*), based on a 99% similarity to the V5-V6 region of the 16*S* rRNA gene in the SILVA 138 database to match the 784F/1061R primer pair used (*72*). Mitochondria and chloroplast reads were filtered out. Analyses and graphs were performed using RStudio version 2022.02.2 and the phyloseq package (*73*). Metadata file, taxonomy table, phylogenetic tree, and ASV table were imported into R to create a phyloseq object. Contaminant ASVs, arising from kit reagents and sample manipulation, were identified using the package decontam (*74*). The function "isNotContaminant" was used as it is more stringent and more adequate for low-biomass samples. One replicate for the Adult F1 condition was removed because of heavy contamination. It is worth noting that bacteria belonging to the *Brachybacterium* genus accounted for more than 90% of the contamination (table S2), which were contaminants of a Qiagen PCR kit.

Genome amplification of LCM samples and shotgun sequencing

To reach sufficient quantities for shotgun sequencing, DNA samples obtained through LCM needed to be amplified. Whole-genome amplification was carried out using the SeqPlex DNA Amplification Kit (Sigma-Aldrich, USA), which is specifically designed for low-quantity, fragmented samples. The same DNA samples that were used for 16*S* rRNA gene metabarcoding were used, and for each generation, 1.5 μl of each of the three replicates was pooled before amplification. For each of the F1 and F2 generations of the F1_6 genotype, one sample containing CAMA DNA from three branches was processed. Amplification was performed according to the manufacturer′s instructions, using 29 cycles in an end-point PCR. Intermediate DNA concentrations were measured using a Qubit fluorometer and a Qubit high-sensitivity double-stranded DNA quantification assay. Primer removal was also carried out using the SeqPlex DNA Amplification Kit. Final DNA quality and quantities were checked on TapeStation (Agilent, USA). 16*S* rRNA gene metabarcoding of the amplified samples showed similar results to the nonamplified samples, confirming that amplification bias was minimal (table S3A).

Samples were then sent to the Ramaciotti Centre for Genomics (Sydney, Australia) for sequencing. Library preparation was performed with a NextFLEX Rapid DNA Seq 2.0 Prep kit and sequenced on a NovaSeq 6000 SP 2 × 100 bp Flowcell Illumina platform.

Data analysis of metagenomics

Each sample was run on two different lanes, so reads from each lane were first merged, according to their direction (i.e., forward reads from both lanes were merged, and reverse reads from both lanes were merged). Adapters were removed from the raw data using Cutadapt v4.0 (*70*) with default settings. Quality control was performed using FastQC v0.11.9 (*75*), and low-quality sequences (phred score < 30) were trimmed using Trimmomatic v0.36 (*76*) (LEADING:30 HEADCROP:10 MINLEN:70). High-quality reads were mapped against a *P. acuta* draft genome (*77*) using Bowtie2 v2.4.5 with default parameters (*78*) to remove host-related reads from the metagenome. Mapped reads were then removed using Samtools v1.11 (*79*). Only paired-end host-removed reads were used for metagenome assembly. Metagenome assembly was carried out using MEGAHIT v1.2.9 (*80*) with a minimum contig length of 1000 bp and the following k-mers: 21, 33, 55, and 77. Contigs from k-mer 77 were used for all downstream processing. Trimmed reads were then mapped back to the assembly using Samtools v1.11 (*79*). Assembled contigs were binned using the binning (with metabat2, concoct, and maxbin2 tools) and bin_refinement (with >70% completeness and <10% contamination as cutoff parameters) modules of MetaWRAP v1.3.2 (*81*). Bin quality and taxonomy were assessed using CheckM2 v0.1.3 (*82*) and GTDB-Tk v2.1.0 (*83*), respectively. These bins were reassembled to further improve the contiguity and bin completeness and contamination stats using the reassemble_bins module SPAdes implemented in MetaWRAP v1.3.2. The final taxonomy of individual contigs on a per-bin level was assessed using CAT/BAT v5.2.3 (*84*), and any contig belonging to a different phylum than the taxonomy assigned

by GTDB-Tk was manually removed. Bin coverage was obtained using CoverM v0.6.1 (https://github.com/wwood/CoverM) using the "genome" option.

Genome annotation

Gene prediction and annotation of bins were performed using Prokka v1.14.6 with default settings (*85*), RAST v2.0 (*86*), KEGG-mapper Reconstruct (*87*), eggNOG-mapper v2.1.6 with a cutoff *e* value of 1×10^{-5} (*88*) with the eggNOG database v5.0 (*89*), and InterProScan v5.55 with Pfam domain annotations (*90*). For Pac_F2b (*Simkania* MAG), Prokka annotation was performed using the "--protein" option with a well-annotated set of chlamydial genes as initial reference. Secondary metabolites were predicted using antiSMASH v6.1.1 (*91*). For the annotation of DMSP demethylases (DmdABC), conserved domains were double-checked with web-based CD-search using an *e*-value cutoff of 1×10^{-5} (*92*). ANIs and AAIs of all three MAGs were calculated using a genome-based matrix calculator (*93*).

Phylogenetic analyses

16*S* rRNA gene sequences were recovered from MAGs using barrnap as implemented in Prokka. The 16*S* rRNA gene phylogenetic tree of the Endozoicomonadaceae family was constructed using full-length 16*S* rRNA gene sequences from the SILVA v132 database. For Pac_F2a, a full-length 16*S* rRNA gene (1536 bp) was recovered and used for the phylogenetic tree construction. For Pac_F1, two fragments were recovered, of 1129 and 401 bp, respectively, and only the 1129-bp fragment was used. A MAFFT alignment was created using Geneious Prime v2019.1.3. This alignment was used to generate a maximum likelihood phylogenetic tree with 1000 ultrafast bootstraps using IQ-TREE v2.2.0.3 (*94*) with the best model TIM3e+R6, selected by ModelFinder wrapped in IQ-TREE (*95*). Sequences belonging to the *Zookishella* genus were chosen as an outgroup. For the *Endozoicomonas* whole-genome phylogenetic tree, GTDB-Tk v2.1.0 (*83*) was used to create an alignment based on 120 gene markers. Nucleotide sequences were chosen because all the genomes belong to the same genus. The genome of *P. haliclonae* was selected as an outgroup. The reference genomes are listed in table S5. A maximum likelihood phylogenetic tree was constructed on the basis of the alignment with IQ-TREE v2.1.2 (*94*) using the best model LG+F+R3, selected by ModelFinder wrapped in IQ-TREE (*95*), and 1000 ultrafast bootstrap replicates (*96*).

For comparative genome analysis of the Pac_F2b MAG, a dataset of high-quality chlamydial genomes based on Dharamshi *et al.* (*55*) was used. This dataset was complemented by additional chlamydial genomes available on the National Center for Biotechnology Information (NCBI) (last accessed on 1 September 2022). Only genomes with a completeness of >70% [determined with CheckM2 v0.1.3 (*82*)] and ANIs of <95% [determined with FastANI v1.33 (*97*)] were considered for the final dataset, which included 139 chlamydial genomes (table S5B). For further comparative analysis of the chlamydial genomes, all encoded protein sequences were clustered into orthologous groups with OrthoFinder v2.5.2 with default parameters (*98*). To obtain the phylogenetic affiliation of the Pac_F2b MAG, a set of concatenated protein sequences from 15 nonsupervised orthologous groups (NOGs) was used (table S10) (*55*). It has been shown previously that the usage of these 15 NOGs retrieves the same topology for chlamydial phylogeny as the application of larger protein sets (*55*). Thus, the dataset from Dharamshi *et al.* (*55*) including a large outgroup of other members of the Planctomycetes, Verrucomicobia, Chlamydiae (PVC) superphylum was expanded by the Pac_F2b MAG and the additional genomes from NCBI. Proteins of these genomes belonging to the 15 NOGs were aligned to the existing alignments from Dharamshi *et al.* (*55*) with MAFFT v7.490 "--add" (*99*). The resulting single protein alignments were subsequently trimmed with BMGE v1.12 (*100*) (entropy 0.6) and concatenated. Maximum likelihood phylogeny was inferred with IQ-TREE v2.1.2 (*94*) with 1000 ultrafast bootstrap replicates (*96*) and 1000 replicates of the SH-like approximate likelihood ratio test (*101*) under the LG+C60+F+R4 model.

Supplementary Materials

This PDF file includes:

Figs. S1 to S14
Legends for tables S1, S3 to S6, S8, and S9
Tables S2, S7, and S10
Legends for datasets S1 to S3

Other Supplementary Material for this manuscript includes the following:

Tables S1, S3 to S6, S8, and S9
Datasets S1 to S3

View/request a protocol for this paper from *Bio-protocol*.

REFERENCES AND NOTES

1. R. Fisher, R. A. O'Leary, S. Low-Choy, K. Mengersen, N. Knowlton, R. E. Brainard, M. J. Caley, Species richness on coral reefs and the pursuit of convergent global estimates. *Curr. Biol.* **25**, 500–505 (2015).
2. D. L. Santavy, C. L. Horstmann, L. M. Sharpe, S. H. Yee, P. Ringold, What is it about coral reefs? Translation of ecosystem goods and services relevant to people and their well-being. *Ecosphere* **12**, e03639 (2021).
3. D. G. Bourne, K. M. Morrow, N. S. Webster, Insights into the coral microbiome: Underpinning the health and resilience of reef ecosystems. *Annu. Rev. Microbiol.* **70**, 317–340 (2016).
4. M. J. H. van Oppen, L. L. Blackall, Coral microbiome dynamics, functions and design in a changing world. *Nat. Rev. Microbiol.* **17**, 557–567 (2019).
5. J. Maire, P. Buerger, W. Y. Chan, P. Deore, A. M. Dungan, M. R. Nitschke, M. J. H. van Oppen, Effects of ocean warming on the underexplored members of the coral microbiome. *Integr. Comp. Biol.* **62**, 1700–1709 (2022).
6. M. R. Nitschke, S. L. Rosset, C. A. Oakley, S. G. Gardner, E. F. Camp, D. J. Suggett, S. K. Davy, The diversity and ecology of Symbiodiniaceae: A traits-based review, in *Advances in Marine Biology* (Academic Press, 2022), pp. 55–127.
7. K. B. Ritchie, Regulation of microbial populations by coral surface mucus and mucus-associated bacteria. *Mar. Ecol. Prog. Ser.* **322**, 1–14 (2006).
8. J. Ceh, M. R. Kilburn, J. B. Cliff, J.-B. Raina, M. van Keulen, D. G. Bourne, Nutrient cycling in early coral life stages: *Pocillopora damicornis* larvae provide their algal symbiont (*Symbiodinium*) with nitrogen acquired from bacterial associates. *Ecol. Evol.* **3**, 2393–2400 (2013).
9. M. P. Lesser, C. H. Mazel, M. Y. Gorbunov, P. G. Falkowski, Discovery of symbiotic nitrogen-fixing cyanobacteria in corals. *Science* **305**, 997–1000 (2004).
10. K. Tandon, C.-Y. Lu, P.-W. Chiang, N. Wada, S.-H. Yang, Y.-F. Chan, P.-Y. Chen, H.-Y. Chang, Y.-J. Chiou, M.-S. Chou, W.-M. Chen, S.-L. Tang, Comparative genomics: Dominant coral-bacterium *Endozoicomonas acroporae* metabolizes dimethylsulfoniopropionate (DMSP). *ISME J.* **14**, 1290–1303 (2020).
11. J. Maire, L. L. Blackall, M. J. H. van Oppen, Intracellular bacterial symbionts in corals: Challenges and future directions. *Microorganisms* **9**, 2209 (2021).
12. E. C. Peters, A survey of cellular reactions to environmental stress and disease in Caribbean scleractinian corals. *Helgol. Meeresunters.* **37**, 113–137 (1984).
13. E. C. Peters, J. J. Oprandy, P. P. Yevich, Possible causal agent of "white band disease" in Caribbean acroporid corals. *J. Invertebr. Pathol.* **41**, 394–396 (1983).

14. T. D. Ainsworth, M. Fine, L. L. Blackall, O. Hoegh-Guldberg, Fluorescence in situ hybridization and spectral imaging of coral-associated bacterial communities. *Appl. Environ. Microbiol.* **72**, 3016–3020 (2006).
15. T. D. Ainsworth, O. Hoegh-Guldberg, Bacterial communities closely associated with coral tissues vary under experimental and natural reef conditions and thermal stress. *Aquat. Biol.* **4**, 289–296 (2009).
16. T. Bayer, M. J. Neave, A. Alsheikh-Hussain, M. Aranda, L. K. Yum, T. Mincer, K. Hughen, A. Apprill, C. R. Voolstra, The microbiome of the Red Sea coral *Stylophora pistillata* is dominated by tissue-associated *Endozoicomonas* bacteria. *Appl. Environ. Microbiol.* **79**, 4759–4762 (2013).
17. M. La Rivière, M. Garel, M. Bally, Localization of endobacteria in the gastrodermis of a Mediterranean gorgonian coral, *Paramuricea clavata*, using fluorescence in situ hybridization. *Mar. Biol.* **163**, 206 (2016).
18. M. J. McKinstry, G. B. Chapman, D. M. Spoon, E. C. Peters, The occurrence of bacterial colonies in the epidermis of the tentacles of the sea anemone *Aiptasia pallida* (Anthozoa: Actinaria). *Trans. Am. Microsc. Soc.* **108**, 239 (1989).
19. M. J. Neave, R. Rachmawati, L. Xun, C. T. Michell, D. G. Bourne, A. Apprill, C. R. Voolstra, Differential specificity between closely related corals and abundant *Endozoicomonas* endosymbionts across global scales. *ISME J.* **11**, 186–200 (2017).
20. E. E. Palincsar, W. R. Jones, J. S. Palincsar, M. A. Glogowski, J. L. Mastro, Bacterial aggregates within the epidermis of the sea anemone *Aiptasia pallida*. *Biol. Bull.* **177**, 130–140 (1989).
21. N. Wada, M.-T. Hsu, K. Tandon, S. S.-Y. Hsiao, H.-J. Chen, Y.-H. Chen, P.-W. Chiang, S.-P. Yu, C.-Y. Lu, Y.-J. Chiou, Y.-C. Tu, X. Tian, B.-C. Chen, D.-C. Lee, H. Yamashiro, D. G. Bourne, S.-L. Tang, High-resolution spatial and genomic characterization of coral-associated microbial aggregates in the coral *Stylophora pistillata*. *Sci. Adv.* **8**, eabo2431 (2022).
22. N. Wada, M. Ishimochi, T. Matsui, F. J. Pollock, S.-L. Tang, T. D. Ainsworth, B. L. Willis, N. Mano, D. G. Bourne, Characterization of coral-associated microbial aggregates (CAMAs) within tissues of the coral *Acropora hyacinthus*. *Sci. Rep.* **9**, 14662 (2019).
23. T. Work, G. Aeby, Microbial aggregates within tissues infect a diversity of corals throughout the Indo-Pacific. *Mar. Ecol. Prog. Ser.* **500**, 1–9 (2014).
24. M. J. Neave, A. Apprill, C. Ferrier-Pagès, C. R. Voolstra, Diversity and function of prevalent symbiotic marine bacteria in the genus *Endozoicomonas*. *Appl. Microbiol. Biotechnol.* **100**, 8315–8324 (2016).
25. C. Pogoreutz, C. A. Oakley, N. Rädecker, A. Cárdenas, G. Perna, N. Xiang, L. Peng, S. K. Davy, D. K. Ngugi, C. R. Voolstra, Coral holobiont cues prime *Endozoicomonas* for a symbiotic lifestyle. *ISME J.* **16**, 1883–1895 (2022).
26. M. J. Neave, C. T. Michell, A. Apprill, C. R. Voolstra, *Endozoicomonas* genomes reveal functional adaptation and plasticity in bacterial strains symbiotically associated with diverse marine hosts. *Sci. Rep.* **7**, 40579 (2017).
27. H. A. Smith, A. Moya, N. E. Cantin, M. J. H. van Oppen, G. Torda, Observations of simultaneous sperm release and larval planulation suggest reproductive assurance in the coral *Pocillopora acuta*. *Front. Mar. Sci.* **6**, 362 (2019).
28. K. Damjanovic, P. Menéndez, L. L. Blackall, M. J. H. van Oppen, Mixed-mode bacterial transmission in the common brooding coral *Pocillopora acuta*. *Environ. Microbiol.* **22**, 397–412 (2020).
29. T. D. Haydon, J. R. Seymour, J. B. Raina, J. Edmondson, N. Siboni, J. L. Matthews, E. F. Camp, D. J. Suggett, Rapid shifts in bacterial communities and homogeneity of symbiodiniaceae in colonies of *Pocillopora acuta* transplanted between reef and mangrove environments. *Front. Microbiol.* **12**, 756091 (2021).
30. C. Dehio, M. Meyer, J. Berger, H. Schwarz, C. Lanz, Interaction of *Bartonella henselae* with endothelial cells results in bacterial aggregation on the cell surface and the subsequent engulfment and internalisation of the bacterial aggregate by a unique structure, the invasome. *J. Cell Sci.* **110**, 2141–2154 (1997).
31. K. Ide, Y. Nakano, M. Ito, Y. Nishikawa, H. Fujimura, H. Takeyama, The effect of co-culture of two coral species on their bacterial composition under captive environments. *Mar. Biotechnol.* **24**, 871–881 (2022).
32. K. Damjanovic, L. L. Blackall, L. M. Peplow, M. J. H. van Oppen, Assessment of bacterial community composition within and among *Acropora loripes* colonies in the wild and in captivity. *Coral Reefs* **39**, 1245–1255 (2020).
33. K. Damjanovic, L. L. Blackall, P. Menéndez, M. J. H. van Oppen, Bacterial and algal symbiont dynamics in early recruits exposed to two adult coral species. *Coral Reefs* **39**, 189–202 (2020).
34. L. Schreiber, K. U. Kjeldsen, P. Funch, J. Jensen, M. Obst, S. López-Legentil, A. Schramm, Endozoicomonas are specific, facultative symbionts of sea squirts. *Front. Microbiol.* **7**, (2016).
35. P. Katharios, H. M. B. Seth-Smith, A. Fehr, J. M. Mateos, W. Qi, D. Richter, L. Nufer, M. Ruetten, M. Guevara Soto, U. Ziegler, N. R. Thomson, R. Schlapbach, L. Vaughan, Environmental marine pathogen isolation using mesocosm culture of sharpsnout seabream: Striking genomic and morphological features of novel Endozoicomonas sp. *Sci. Rep.* **5**, 17609 (2015).
36. F. U. Zielinski, A. Pernthaler, S. Duperron, L. Raggi, O. Giere, C. Borowski, N. Dubilier, Widespread occurrence of an intranuclear bacterial parasite in vent and seep bathymodiolin mussels. *Environ. Microbiol.* **11**, 1150–1167 (2009).
37. A. Collingro, S. Köstlbacher, M. Horn, Chlamydiae in the environment. *Trends Microbiol.* **28**, 877–888 (2020).
38. W. Y. Chan, L. M. Peplow, P. Menéndez, A. A. Hoffmann, M. J. H. van Oppen, The roles of age, parentage and environment on bacterial and algal endosymbiont communities in *Acropora* corals. *Mol. Ecol.* **28**, 3830–3843 (2019).
39. P. Buerger, R. T. Vanstone, J. Maire, M. J. H. van Oppen, Long-term heat selection of the coral endosymbiont *Cladocopium* C1^{acro} (Symbiodiniaceae) stabilizes associated bacterial communities. *Int. J. Mol. Sci.* **23**, 4913 (2022).
40. J. Maire, S. K. Girvan, S. E. Barkla, A. Perez-Gonzalez, D. J. Suggett, L. L. Blackall, M. J. H. Van Oppen, Intracellular bacteria are common and taxonomically diverse in cultured and in hospite algal endosymbionts of coral reefs. *ISME J.* **15**, 2028–2042 (2021).
41. S. Poppert, A. Essig, R. Marre, M. Wagner, M. Horn, Detection and differentiation of chlamydiae by fluorescence in situ hybridization. *Appl. Environ. Microbiol.* **68**, 4081–4089 (2002).
42. I. Lagkouvardos, J. Shen, M. Horn, Improved axenization method reveals complexity of symbiotic associations between bacteria and acanthamoebae. *Environ. Microbiol. Rep.* **6**, 383–388 (2014).
43. M. I. Blandford, A. Taylor-Brown, T. A. Schlacher, B. Nowak, A. Polkinghorne, Epitheliocystis in fish: An emerging aquaculture disease with a global impact. *Transbound. Emerg. Dis.* **65**, 1436–1446 (2018).
44. L. Weber, P. Gonzalez-Díaz, M. Armenteros, A. Apprill, The coral ecosphere: A unique coral reef habitat that fosters coral–microbial interactions. *Limnol. Oceanogr.* **64**, 2373–2388 (2019).
45. S. Köstlbacher, A. Collingro, T. Halter, F. Schulz, S. P. Jungbluth, M. Horn, Pangenomics reveals alternative environmental lifestyles among chlamydiae. *Nat. Commun.* **12**, 4021 (2021).
46. D. G. Bourne, C. B. Munn, Diversity of bacteria associated with the coral *Pocillopora damicornis* from the Great Barrier Reef. *Environ. Microbiol.* **7**, 1162–1174 (2005).
47. X. Wang, H. Zhou, H. Chen, X. Jing, W. Zheng, R. Li, T. Sun, J. Liu, J. Fu, L. Huo, Y. Li, Y. Shen, X. Ding, R. Müller, X. Bian, Y. Zhang, Discovery of recombinases enables genome mining of cryptic biosynthetic gene clusters in Burkholderiales species. *Proc. Natl. Acad. Sci. U.S.A.* **115**, E4255–E4263 (2018).
48. J. E. Martyn, L. Gomez-Valero, C. Buchrieser, The evolution and role of eukaryotic-like domains in environmental intracellular bacteria: The battle with a eukaryotic cell. *FEMS Microbiol. Rev.* **46**, fuac012 (2022).
49. L. Craig, K. T. Forest, B. Maier, Type IV pili: Dynamics, biophysics and functional consequences. *Nat. Rev. Microbiol.* **17**, 429–440 (2019).
50. V. Michalkova, J. B. Benoit, B. L. Weiss, G. M. Attardo, S. Aksoy, Vitamin B6 generated by obligate symbionts is critical for maintaining proline homeostasis and fecundity in tsetse flies. *Appl. Environ. Microbiol.* **80**, 5844–5853 (2014).
51. M. T. Croft, A. D. Lawrence, E. Raux-Deery, M. J. Warren, A. G. Smith, Algae acquire vitamin B_{12} through a symbiotic relationship with bacteria. *Nature* **438**, 90–93 (2005).
52. J. Maire, M. J. H. van Oppen, A role for bacterial experimental evolution in coral bleaching mitigation? *Trends Microbiol.* **30**, 217–228 (2022).
53. R. S. Peixoto, P. M. Rosado, D. C. d. A. Leite, A. S. Rosado, D. G. Bourne, Beneficial microorganisms for corals (BMC): Proposed mechanisms for coral health and resilience. *Front. Microbiol.* **8**, 341 (2017).
54. M. Szabó, A. W. D. Larkum, I. Vass, A review: The role of reactive oxygen species in mass coral bleaching, in *Advances in Photosynthesis and Respiration* (Springer, 2020), vol. 45, pp. 459–488.
55. J. E. Dharamshi, N. Gaarslev, K. Steffen, T. Martin, D. Sipkema, T. J. G. Ettema, Genomic diversity and biosynthetic capabilities of sponge-associated chlamydiae. *ISME J.* **16**, 2725–2740 (2022).
56. B. M. Dudiak, T. M. Nguyen, D. Needham, T. C. Outlaw, D. G. McCafferty, Inhibition of the futalosine pathway for menaquinone biosynthesis suppresses *Chlamydia trachomatis* infection. *FEBS Lett.* **595**, 2995–3005 (2021).
57. M. Almirón, M. Martínez, N. Sanjuan, R. A. Ugalde, Ferrochelatase is present in *Brucella abortus* and is critical for its intracellular survival and virulence. *Infect. Immun.* **69**, 6225–6230 (2001).
58. N. D. Hammer, M. L. Reniere, J. E. Cassat, Y. Zhang, A. O. Hirsch, M. Indriati Hood, E. P. Skaar, Two heme-dependent terminal oxidases power *Staphylococcus aureus* organ-specific colonization of the vertebrate host. *MBio* **4**, e00241-13 (2013).

59. C. von Eiff, C. Heilmann, R. A. Proctor, C. Woltz, G. Peters, F. Götz, A site-directed *Staphylococcus aureus* hemB mutant is a small-colony variant which persists intracellularly. *J. Bacteriol.* **179**, 4706–4712 (1997).
60. P. Engström, B. D. Nguyen, J. Normark, I. Nilsson, R. J. Bastidas, Å. Gylfe, M. Elofsson, K. A. Fields, R. H. Valdivia, H. Wolf-Watz, S. Bergström, Mutations in *hemG* mediate resistance to salicylidene acylhydrazides, demonstrating a novel link between protoporphyrinogen oxidase (HemG) and *Chlamydia trachomatis* infectivity. *J. Bacteriol.* **195**, 4221–4230 (2013).
61. M. J. Gosalbes, A. Lamelas, A. Moya, A. Latorre, The striking case of tryptophan provision in the cedar aphid *Cinara cedri*. *J. Bacteriol.* **190**, 6026–6029 (2008).
62. J. P. McCutcheon, C. D. von Dohlen, An Interdependent metabolic patchwork in the nested symbiosis of mealybugs. *Curr. Biol.* **21**, 1366–1372 (2011).
63. M. Ziegler, C. G. B. Grupstra, M. M. Barreto, M. Eaton, J. BaOmar, K. Zubier, A. Al-Sofyani, A. J. Turki, R. Ormond, C. R. Voolstra, Coral bacterial community structure responds to environmental change in a host-specific manner. *Nat. Commun.* **10**, 3092 (2019).
64. H. Daims, A. Brühl, R. Amann, K. H. Schleifer, M. Wagner, The domain-specific probe EUB338 is insufficient for the detection of all bacteria: Development and evaluation of a more comprehensive probe set. *Syst. Appl. Microbiol.* **22**, 434–444 (1999).
65. G. Wallner, R. Amann, W. Beisker, Optimizing fluorescent in situ hybridization with rRNA-targeted oligonucleotide probes for flow cytometric identification of microorganisms. *Cytometry* **14**, 136–143 (1993).
66. J. Maire, N. Parisot, M. Galvao Ferrarini, A. Vallier, B. Gillet, S. Hughes, S. Balmand, C. Vincent-Monégat, A. Zaidman-Rémy, A. Heddi, Spatial and morphological reorganization of endosymbiosis during metamorphosis accommodates adult metabolic requirements in a weevil. *Proc. Natl. Acad. Sci. U.S.A.* **117**, 19347–19358 (2020).
67. L. M. Hartman, M. J. H. van Oppen, L. L. Blackall, Microbiota characterization of *Exaiptasia diaphana* from the great barrier reef. *Anim. Microbiome* **2**, 10 (2020).
68. J. Maire, L. L. Blackall, M. J. H. van Oppen, Microbiome characterization of defensive tissues in the model anemone Exaiptasia diaphana. *BMC Microbiol.* **21**, 152 (2021).
69. E. Bolyen, J. R. Rideout, M. R. Dillon, N. A. Bokulich, C. C. Abnet, G. A. Al-Ghalith, H. Alexander, E. J. Alm, M. Arumugam, F. Asnicar, Y. Bai, J. E. Bisanz, K. Bittinger, A. Brejnrod, C. J. Brislawn, C. T. Brown, B. J. Callahan, A. M. Caraballo-Rodríguez, J. Chase, E. K. Cope, R. Da Silva, C. Diener, P. C. Dorrestein, G. M. Douglas, D. M. Durall, C. Duvallet, C. F. Edwardson, M. Ernst, M. Estaki, J. Fouquier, J. M. Gauglitz, S. M. Gibbons, D. L. Gibson, A. Gonzalez, K. Gorlick, J. Guo, B. Hillmann, S. Holmes, H. Holste, C. Huttenhower, G. A. Huttley, S. Janssen, A. K. Jarmusch, L. Jiang, B. D. Kaehler, K. B. Kang, C. R. Keefe, P. Keim, S. T. Kelley, D. Knights, I. Koester, T. Kosciolek, J. Kreps, M. G. I. Langille, J. Lee, R. Ley, Y. X. Liu, E. Loftfield, C. Lozupone, M. Maher, C. Marotz, B. D. Martin, D. McDonald, L. J. McIver, A. V. Melnik, J. L. Metcalf, S. C. Morgan, J. T. Morton, A. T. Naimey, J. A. Navas-Molina, L. F. Nothias, S. B. Orchanian, T. Pearson, S. L. Peoples, D. Petras, M. L. Preuss, E. Pruesse, L. B. Rasmussen, A. Rivers, M. S. Robeson, P. Rosenthal, N. Segata, M. Shaffer, A. Shiffer, R. Sinha, S. J. Song, J. R. Spear, A. D. Swafford, L. R. Thompson, P. J. Torres, P. Trinh, A. Tripathi, P. J. Turnbaugh, S. Ul-Hasan, J. J. J. van der Hooft, F. Vargas, Y. Vázquez-Baeza, E. Vogtmann, M. von Hippel, W. Walters, Y. Wan, M. Wang, J. Warren, K. C. Weber, C. H. D. Williamson, A. D. Willis, Z. Z. Xu, J. R. Zaneveld, Y. Zhang, Q. Zhu, R. Knight, J. G. Caporaso, Reproducible, interactive, scalable and extensible microbiome data science using QIIME 2. *Nat. Biotechnol.* **37**, 852–857 (2019).
70. M. Martin, Cutadapt removes adapter sequences from high-throughput sequencing reads. *EMBnet j.* **17**, 10 (2011).
71. B. J. Callahan, P. J. McMurdie, M. J. Rosen, A. W. Han, A. J. A. Johnson, S. P. Holmes, DADA2: High-resolution sample inference from Illumina amplicon data. *Nat. Methods* **13**, 581–583 (2016).
72. N. A. Bokulich, B. D. Kaehler, J. R. Rideout, M. Dillon, E. Bolyen, R. Knight, G. A. Huttley, J. Gregory Caporaso, Optimizing taxonomic classification of marker-gene amplicon sequences with QIIME 2's q2-feature-classifier plugin. *Microbiome* **6**, 90 (2018).
73. P. J. McMurdie, S. Holmes, phyloseq: An R package for reproducible interactive analysis and graphics of microbiome census data. *PLOS ONE* **8**, e61217 (2013).
74. N. M. Davis, D., M. Proctor, S. P. Holmes, D. A. Relman, B. J. Callahan, Simple statistical identification and removal of contaminant sequences in marker-gene and metagenomics data. *Microbiome* **6**, 226 (2018).
75. S. Andrews, FASTQC. A quality control tool for high throughput sequence data|BibSonomy (2010); www.bibsonomy.org/bibtex/f230a919c34360709aa298734d63dca3.
76. A. M. Bolger, M. Lohse, B. Usadel, Trimmomatic: A flexible trimmer for Illumina sequence data. *Bioinformatics* **30**, 2114–2120 (2014).
77. J. Vidal-Dupiol, C. Chaparro, M. Pratlong, P. Pontarotti, C. Grunau, G. Mitta, Sequencing, de novo assembly and annotation of the genome of the scleractinian coral, *Pocillopora acuta*. bioRxiv 698688 [Preprint]. 19 April 2020. https://doi.org/10.1101/698688.
78. B. Langmead, S. L. Salzberg, Fast gapped-read alignment with Bowtie 2. *Nat. Methods* **9**, 357–359 (2012).
79. H. Li, B. Handsaker, A. Wysoker, T. Fennell, J. Ruan, N. Homer, G. Marth, G. Abecasis, R. Durbin, The sequence alignment/map format and SAMtools. *Bioinformatics* **25**, 2078–2079 (2009).
80. D. Li, C. M. Liu, R. Luo, K. Sadakane, T. W. Lam, MEGAHIT: An ultra-fast single-node solution for large and complex metagenomics assembly via succinct de Bruijn graph. *Bioinformatics* **31**, 1674–1676 (2015).
81. G. V. Uritskiy, J. Diruggiero, J. Taylor, MetaWRAP—A flexible pipeline for genome-resolved metagenomic data analysis. *Microbiome* **6**, 158 (2018).
82. A. Chklovski, D. H. Parks, B. J. Woodcroft, G. W. Tyson, CheckM2: A rapid, scalable and accurate tool for assessing microbial genome quality using machine learning. bioRxiv 2022.07.11.499243 [Preprint]. 11 July 2022. https://doi.org/10.1101/2022.07.11.499243.
83. P.-A. Chaumeil, A. J. Mussig, P. Hugenholtz, D. H. Parks, GTDB-Tk: A toolkit to classify genomes with the Genome Taxonomy Database. *Bioinformatics* **36**, 1925–1927 (2020).
84. F. A. B. Von Meijenfeldt, K. Arkhipova, D. D. Cambuy, F. H. Coutinho, B. E. Dutilh, Robust taxonomic classification of uncharted microbial sequences and bins with CAT and BAT. *Genome Biol.* **20**, 217 (2019).
85. T. Seemann, Prokka: Rapid prokaryotic genome annotation. *Bioinformatics* **30**, 2068–2069 (2014).
86. R. K. Aziz, D. Bartels, A. A. Best, M. DeJongh, T. Disz, R. A. Edwards, K. Formsma, S. Gerdes, E. M. Glass, M. Kubal, F. Meyer, G. J. Olsen, R. Olson, A. L. Osterman, R. A. Overbeek, L. K. McNeil, D. Paarmann, T. Paczian, B. Parrello, G. D. Pusch, C. Reich, R. Stevens, O. Vassieva, V. Vonstein, A. Wilke, O. Zagnitko, The RAST server: Rapid annotations using subsystems technology. *BMC Genomics* **9**, 75 (2008).
87. M. Kanehisa, Y. Sato, KEGG mapper for inferring cellular functions from protein sequences. *Protein Sci.* **29**, 28–35 (2020).
88. C. P. Cantalapiedra, A. Hernández-Plaza, I. Letunic, P. Bork, J. Huerta-Cepas, eggNOG-mapper v2: Functional annotation, orthology assignments, and domain prediction at the metagenomic scale. *Mol. Biol. Evol.* **38**, 5825–5829 (2021).
89. J. Huerta-Cepas, D. Szklarczyk, D. Heller, A. Hernández-Plaza, S. K. Forslund, H. Cook, D. R. Mende, I. Letunic, T. Rattei, L. J. Jensen, C. von Mering, P. Bork, eggNOG 5.0: A hierarchical, functionally and phylogenetically annotated orthology resource based on 5090 organisms and 2502 viruses. *Nucleic Acids Res.* **47**, D309–D314 (2019).
90. P. Jones, D. Binns, H. Y. Chang, M. Fraser, W. Li, C. McAnulla, H. McWilliam, J. Maslen, A. Mitchell, G. Nuka, S. Pesseat, A. F. Quinn, A. Sangrador-Vegas, M. Scheremetjew, S. Y. Yong, R. Lopez, S. Hunter, InterProScan 5: Genome-scale protein function classification. *Bioinformatics* **30**, 1236–1240 (2014).
91. K. Blin, S. Shaw, A. M. Kloosterman, Z. Charlop-Powers, G. P. Van Wezel, M. H. Medema, T. Weber, antiSMASH 6.0: Improving cluster detection and comparison capabilities. *Nucleic Acids Res.* **49**, W29–W35 (2021).
92. A. Marchler-Bauer, S. H. Bryant, CD-Search: Protein domain annotations on the fly. *Nucleic Acids Res.* **32**, W327–W331 (2004).
93. L. M. Rodriguez-R, K. T. Konstantinidis, The enveomics collection: A toolbox for specialized analyses of microbial genomes and metagenomes. *PeerJ* **4**, e1900v1 (2016).
94. B. Q. Minh, H. A. Schmidt, O. Chernomor, D. Schrempf, M. D. Woodhams, A. von Haeseler, R. Lanfear, IQ-TREE 2: New models and efficient methods for phylogenetic inference in the genomic era. *Mol. Biol. Evol.* **37**, 1530–1534 (2020).
95. S. Kalyaanamoorthy, B. Q. Minh, T. K. F. Wong, A. von Haeseler, L. S. Jermiin, ModelFinder: Fast model selection for accurate phylogenetic estimates. *Nat. Methods* **14**, 587–589 (2017).
96. D. T. Hoang, O. Chernomor, A. von Haeseler, B. Q. Minh, L. S. Vinh, UFBoot2: Improving the ultrafast bootstrap approximation. *Mol. Biol. Evol.* **35**, 518–522 (2018).
97. C. Jain, L. M. Rodriguez-R, A. M. Phillippy, K. T. Konstantinidis, S. Aluru, High throughput ANI analysis of 90K prokaryotic genomes reveals clear species boundaries. *Nat. Commun.* **9**, 5114 (2018).
98. D. M. Emms, S. Kelly, OrthoFinder: Phylogenetic orthology inference for comparative genomics. *Genome Biol.* **20**, 238 (2019).
99. K. Katoh, D. M. Standley, MAFFT multiple sequence alignment software version 7: Improvements in performance and usability. *Mol. Biol. Evol.* **30**, 772–780 (2013).
100. A. Criscuolo, S. Gribaldo, BMGE (Block Mapping and Gathering with Entropy): A new software for selection of phylogenetic informative regions from multiple sequence alignments. *BMC Evol. Biol.* **10**, 210 (2010).
101. S. Guindon, J.-F. Dufayard, V. Lefort, M. Anisimova, W. Hordijk, O. Gascuel, New algorithms and methods to estimate maximum-likelihood phylogenies: Assessing the performance of PhyML 3.0. *Syst. Biol.* **59**, 307–321 (2010).

Acknowledgments: We thank the Biosciences Microscopy Unit (University of Melbourne) and the Biological Optical Microscopy Platform (University of Melbourne) for the use of their confocal microscopes and laser capture dissection, and particularly G. Segal, S. Cheung, and S. Mills for their valuable assistance. We thank the Melbourne Histology Platform (University of

Melbourne), L. Leone, and L. Foster for their assistance with sample sectioning. We also thank the Melbourne Research Cloud and the Life Science Compute Cluster for providing the high-performance computing instances needed for this work. We are grateful to S. Topa and I. Buthgamuwa for their efforts in trying to culture *Endozoicomonas*. The adult parent colonies of *P. acuta* were collected under the Great Barrier Reef Marine Park Authority (GBRMPA) Permit Number G14/36732.1. We acknowledge the Australian Research Council (DP200101613) for funding K.T.'s salary. **Funding:** This work was supported by Australian Research Council Laureate Fellowship FL180100036 (to M.J.H.v.O.), the Paul G. Allen Family Foundation, and Austrian Science Fund grant no. P32112 (to A.C.). **Author contributions:** Conceptualization: J.M., L.L.B., and M.J.H.v.O. Formal analysis: J.M., K.T., A.C., G.K.P., and M.H. Funding acquisition: M.J.H.v.O. and N.E.C. Investigation: J.M., A.v.d.M., K.D., C.R.G., S.S., and N.E.C. Methodology: J.M. Supervision: L.L.B. and M.J.H.v.O. Visualization: J.M., K.T., and A.C. Writing—original draft preparation: J.M. and M.J.H.v.O. All authors have read and edited the manuscript. **Competing interests:** The authors declare that they have no competing interests. **Data and materials availability:** All data needed to evaluate the conclusions in the paper are present in the paper and/or the Supplementary Materials. Raw data are available under NCBI BioProject IDs PRJNA891910 (adult CAMAs, MiSeq and NovaSeq raw data, MAGs) and PRJNA891892 (whole larva microbiome, MiSeq raw data).

Submitted 30 November 2022
Accepted 13 April 2023
Published 17 May 2023
10.1126/sciadv.adg0773